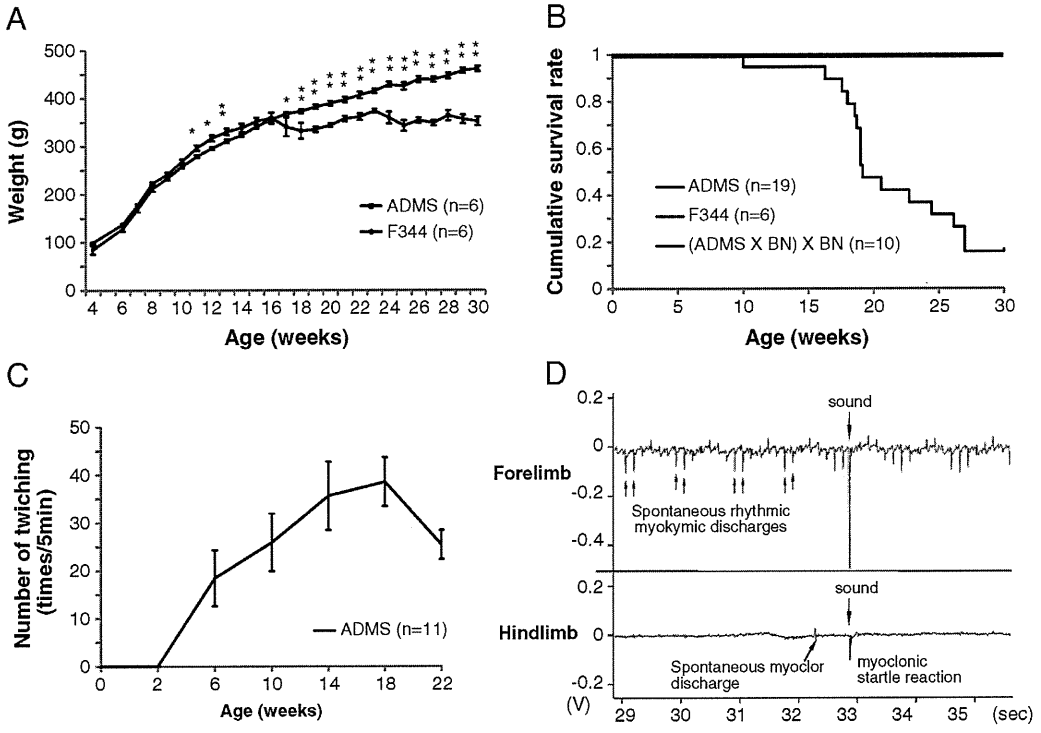

Fig. 1 – Gross and myokymic phenotypes in ADMS rats. (A) Comparison of body weight between ADMS (n=6) and F344 (n=6) rats. ADMS rats show increased body weight from 10 weeks of age, which is then reduced, in conjunction with the severe convulsive seizures from 18 weeks of age. Error bars indicate SEM. Unpaired student's t-test: *p<0.05, **p<0.01. (B) Kaplan–Meier survival curves of ADMS (n=19), F344 (n=6) rats, and (ADMS×BN)×BN backcross progeny (n=10). By 30 weeks of age, 84% of ADMS rats had died. (C) Twitching behaviours appeared from 6 weeks of age and peaked at 18 weeks of age in ADMS rats (n=11). Error bars indicate SEM. (D) Electromyogram (EMG) recording of forelimb and hindlimb muscles during the interictal period in 16-week-old ADMS rats. A spontaneous myoclonic discharge was detected from the hindlimb, as well as a myoclonic startle reaction in response to a sound stimulus. Spontaneous rhythmic myokymic discharges (7 Hz) were detected from the forelimb.

also showed rhythmic multiple discharges with an intra-burst frequency of 7 Hz. This firing pattern is similar to that observed in human myokymia.

2.3. *Spontaneous convulsive seizures in ADMS rats*

ADMS rats exhibited spontaneous convulsive seizures from 10 weeks of age (Fig. 2A). Occurrence of seizures was aggravated during cage changing or animal handling. Seizure onset was observed in all ADMS rats (n=11) by 16 weeks of age. The average number of seizures significantly increased with age until 20 weeks of age (Fig. 2A), while the mean duration of each seizure did not increase (Fig. 2B). The typical seizure phenotype encompassed four stages: (i) initial sudden falling down, (ii) secondly jerking of the entire body or the extremities as clonic phase, occasionally with a tonic phase with stiffening of the entire body, (iii) immobility, and (iv) rearing with muscle twitching (Fig. 2C; Supplementary Video 2). Motor automatisms, such as repetitive chewing, occasionally occurred during the seizure. Cortical and hippocampal EEG recordings identified four characteristic EEG patterns corresponding to the four stages of the seizure phenotype. First, aberrant large spike activity associated with falling-down behaviour (i). Second, low-voltage fast wave discharges detected during the tonic stage, and spike-and-wave discharges (2 Hz) detected during the clonic convulsive stage (ii). These discharges terminated abruptly, followed by fast spikes with low to high voltages in the freezing stage (iii). Finally, polyspike and large wave complexes (1–3 Hz) during the rearing stage (iv). Although cortical and hippocampal EEG recordings were generally synchronized, ictal epileptic activities in the hippocampus tended to precede cortical discharges, specifically at the onset of seizure ((i) initial sudden falling), and/or during the transition stage between freezing (iii) and rearing (iv). The behavioural phenotypes and abnormal discharge patterns in ADMS rats are similar to other rodent models of temporal lobe epilepsy (Rho et al., 1999; Wenzel et al., 2007). These spontaneous convulsive seizures and the twitching phenotypes were significantly prevented 30 min after the administration of carbamazepine (CBZ) in ADMS rats (n=5) (Figs. 2D, E). Histopathological analysis of ADMS rats at 16–19 weeks of age revealed no major abnormalities in haematoxylin staining of the brain (Supplementary Fig. 1).

2.4. *Identification of a Kcna1 S309T mutation*

We crossed ADMS females to BN males, a rat strain suitable for genetic mapping studies, because of their distinct genetic background. We obtained eight F1 progeny exhibiting the

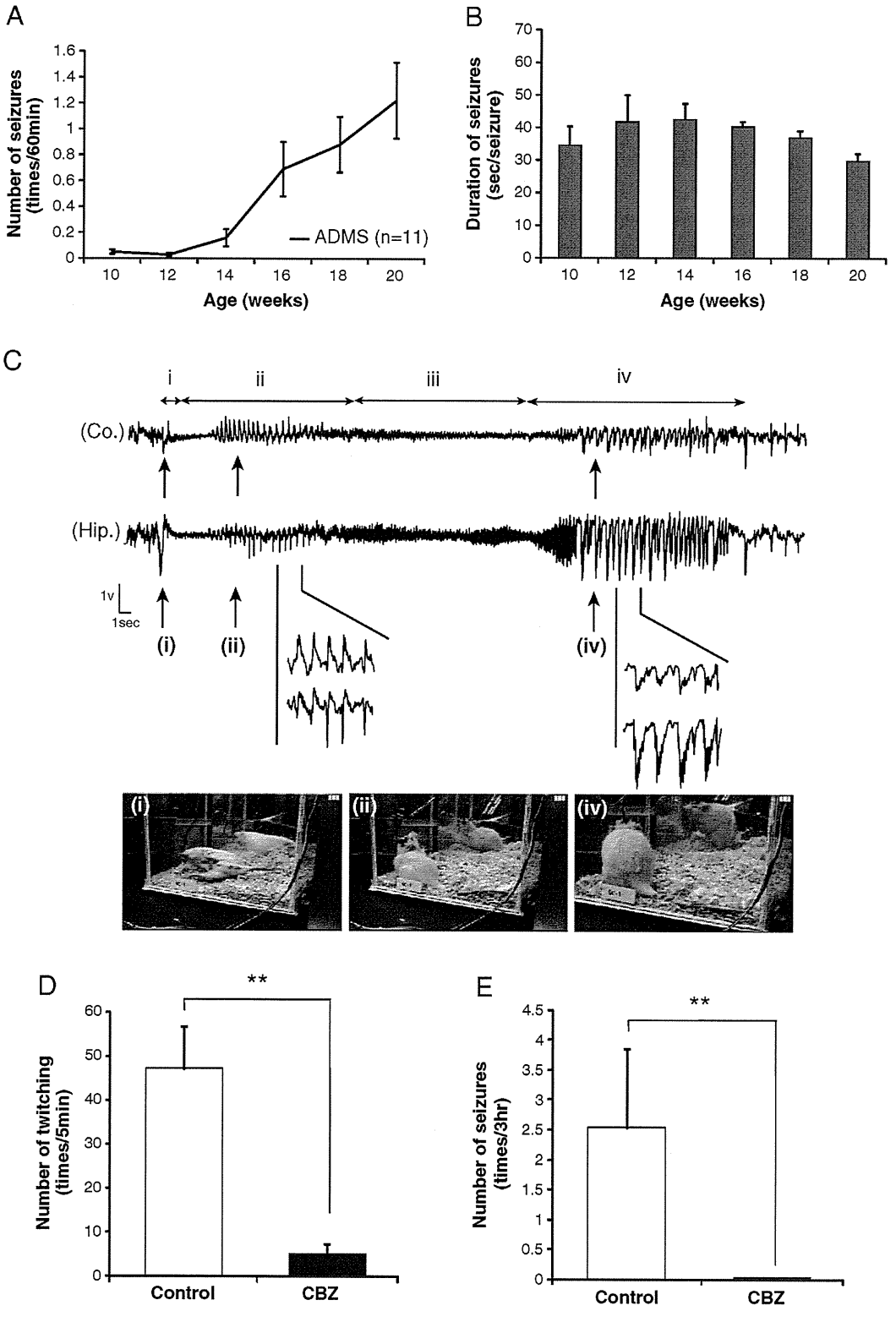

Fig. 2 – Spontaneous epileptic seizures in ADMS rats. (A) Convulsive seizures started from 10 weeks of age and increased in number, peaking at 20 weeks of age in ADMS rats (n=11). Error bars indicate SEM. (B) The mean duration of seizures did not differ between ages. Unpaired student's t-test: $p>0.05$. (C) Cortical (Co.) and hippocampal (Hip.) electroencephalogram (EEG) recorded from an ADMS rat at 16 weeks of age. Although the discharges occurred synchronously in both cortex and hippocampus, the amplitude was higher in hippocampus than in cortex. Behavioural patterns were correlated with EEG events. i: tonic attack; ii: clonus of the limbs; iii: immobility; and iv: rearing with chewing gesture. Photographs show characteristic postures in stages i, ii and iv. (D) The spontaneous convulsive seizures in ADMS rats (n=5) were prevented by the administration of carbamazepine (CBZ). (E) Numbers of the twitching behaviours in ADMS rats (n=5) were significantly decreased by CBZ. Paired student's t-test: $^{**}p<0.01$.

same abnormal behaviours as the ADMS rats, albeit with a slightly delayed onset. Muscle twitching was observed from 10 to 12 weeks of age, compared with 6 weeks in ADMS rats, while spontaneous convulsive seizures were not evident until 20–30 weeks of age in four animals, with the remaining four animals not presenting with seizures until 40 weeks, suggesting modifier gene(s) are associated with the onset of seizures. Further breeding, generated 180 (ADMS×BN)×BN

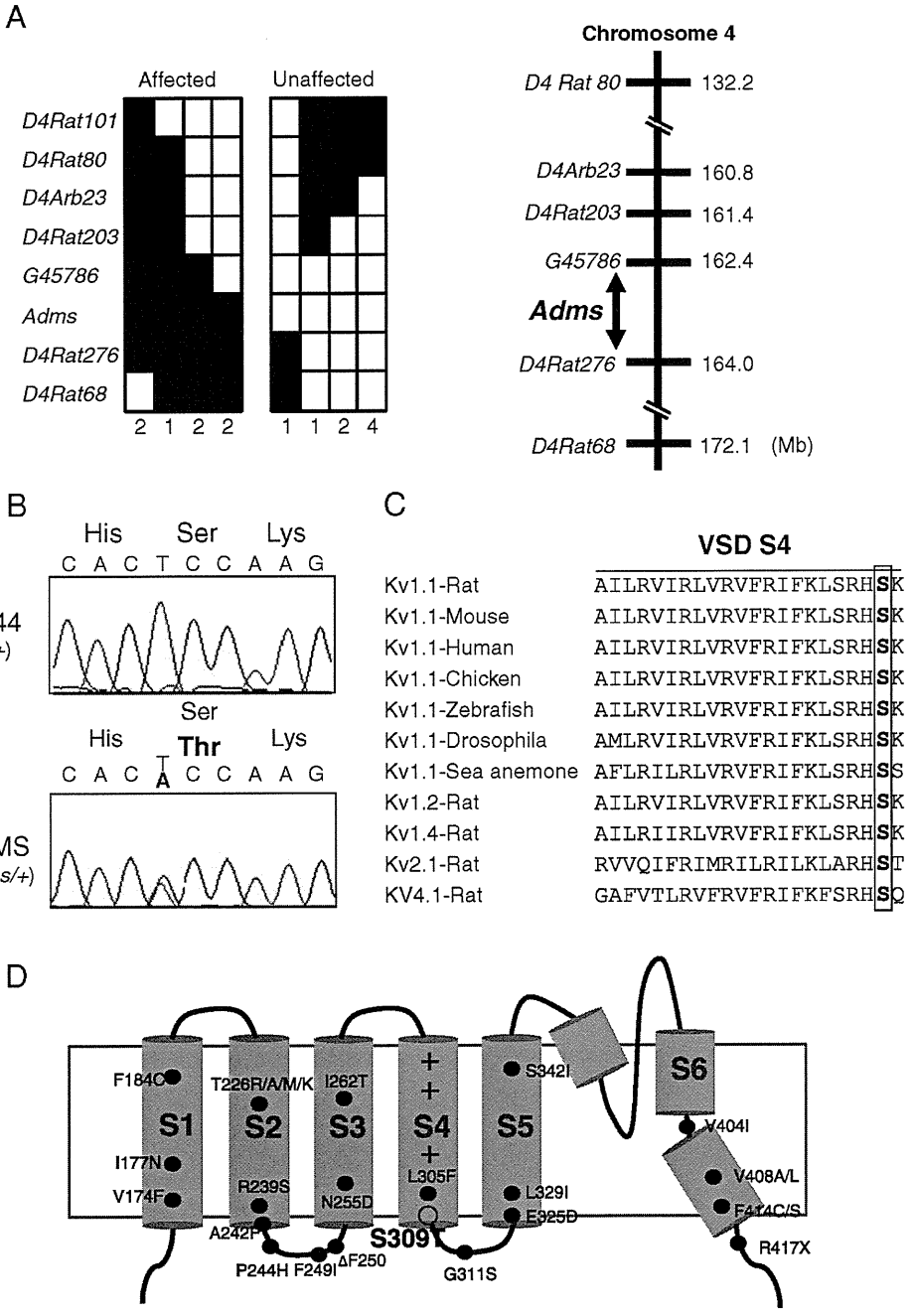

Fig. 3 – Identification of *Adms* mutation. (A) (Left) Distribution of haplotypes in (ADMS×BN)×BN backcross progeny, determined using SSLP markers from rat chromosome 4. White boxes represent BN homozygous alleles or 'unaffected' for *Adms*. Black boxes represent F344-derived heterozygotes or 'affected' alleles. Numbers of the backcross progeny are depicted at the bottom of the haplotypes. (Right) *Adms* was mapped to a 1.6-Mb region between *G45786* and *D4Rat276*. (B) Sequencing analysis in F344 (upper) and ADMS (lower) rats revealed a nucleotide change from T to A (arrowhead) located at position 925 of the *Kcna1* gene. The mutation results in an amino acid substitution of serine (Ser) with threonine (Thr) at codon 309 of the KCNA1 protein. (C) Amino acid sequence alignment of the voltage-sensor domain S4 of KCNA1 in several species and between KCNA families. The S309T amino acid substitution (boxed) is located in a region highly conserved among species and within the KCNA family. (D) Schematic representation of the Kv1.1 subunit. Black circles represent the positions of the EA1 mutations thus far reported and a white circle represents the rat *Adms* mutation.

backcross progeny, with 87 rats expressing the twitching phenotype at 10–14 weeks of age, and seizure activity from 20 weeks of age.

Genome-wide scanning using 121 SSLP markers mapped the *Adms* locus to a 1.6-Mb genomic region, between markers G45786 and D4Rat276 on Chr 4 (Fig. 3A). Eighteen known or predicted genes within the *Adms* region were obtained from the Ensembl database (http://www.ensembl.org). Among them were the voltage-gated potassium channel families, *Kcna1*, *Kcna5*, and *Kcna6*, that we deemed to be good candidates, based on their functional ability to regulate membrane potential, neuronal excitability, and nerve signalling (Johnston et al., 2010; Wulff et al., 2009). In particular, the behavioural phenotypes of ADMS rats were similar to those of *Kcna1*-deficient mice (Smart et al., 1998), and to the symptoms reported in human EA1 (Pessia and Hanna, 1993; Rajakulendran et al., 2007). We compared the sequences of *Kcna1*, *Kcna5*, and *Kcna6* between F344 and ADMS rats, and identified a T-to-A mutation at nucleotide 925 of the *Kcna1* gene, but no mutations in *Kcna5* and *Kcna6* genes (Fig. 3B). The T925A mutation of *Kcna1* results in a substitution of serine for threonine at residue 309, which is located in the voltage sensor segment, S4, of Kv1.1. This residue is highly conserved among species and other potassium channel family genes (Fig. 3C). To date, more than 20 *KCNA1* mutations have been reported in EA1 patients (Bretschneider et al., 1999; Browne et al., 1994; Browne et al., 1995; Chen et al., 2007; Comu et al., 1996; Demos et al., 2009; Eunson et al., 2000; Glaudemans et al., 2009b; Graves et al., 2010; Imbrici et al., 2008; Kinali et al., 2004; Klein et al., 2004; Knight et al., 2000; Lee et al., 2004; Poujois et al., 2006; Scheffer et al., 1998; Shook et al., 2008; Zerr et al., 1998; Zuberi et al., 1999) (Fig. 3D). Interestingly, the *KCNA1* missense mutation L305F, which is closely located to S309T in the S4 segment, was reported in an EA1 family uniquely exhibiting brief episodes of cerebellar ataxia in early childhood and progressive development of chronic neuromyotonia with muscle rippling and hypertrophy (Poujois et al., 2006).

2.5. *Premature death of homozygous S309T rats*

To investigate the effect of the homozygous mutation of *Kcna1* S309T, we crossed N10 heterozygous ADMS males and females. The behaviour and appearance of homozygous S309T/S309T rats at birth did not differ from those of heterozygous S309T/+ and WT+/+ littermates. Western blot analysis showed that the expression level of endogenous KCNA1 protein in the brain did not differ between homozygous, heterozygous and WT littermate rats (Supplementary Fig. 2). However, from postnatal day 14, development of the homozygous rats was dramatically impaired and body weight significantly decreased compared with heterozygous and WT littermates (Fig. 4A). In conjunction with reduced body weight, the homozygous rats showed tremors, motor incoordination, mainly caused by extension of hind limbs, and spontaneous convulsive seizures (Supplementary Video 3). These phenotypes progressively worsen with age. Homozygous pups became inactive except during seizures, and usually remained isolated from their mother. All homozygous rats died prematurely with a mean lifetime of 16 days (Fig. 4B).

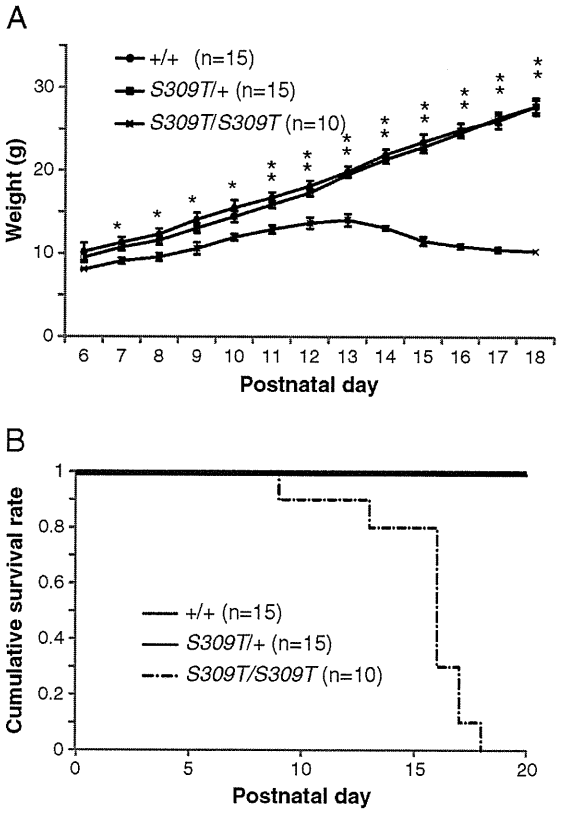

Fig. 4 – Lethality of homozygous S309T rats. (A) From postnatal (P) 7 days, the body weight of homozygous S309T/S309T rats (n=10) was significantly reduced compared with heterozygous S309T/+ (n=15) and WT+/+ (n=15) rats. Error bars indicate SEM. Unpaired student's t-test: *p<0.05, **p<0.01. (B) Kaplan–Meier survival curves of homozygous S309T/S309T (n=10), heterozygous S309T/+ (n=15) and WT+/+ (n=15) rats. All homozygous rats had died by P18.

No homozygous rats survived beyond postnatal day 18, while neither heterozygous or WT littermates died at this age. Post-mortem examination of homozygous rats detected an absence of stomach contents, suggesting early mortality might result from feeding failure partially caused by the severe behavioural phenotypes.

2.6. *Motor incoordination by cold-swim tests*

To examine whether ADMS rats show cold-swim induced neuromyotonia and motor incoordination that were recognized in *Kcna1*-deficient mice (Zhou et al., 1998), we forced rats to swim in a tank filled with either warm (38 °C) or cold (17 °C) water. We used 5-week-old ADMS rats that have never exhibited muscle twitching or spontaneous seizures. In warm water, there was no behavioural difference between ADMS and WT rats during 2-min swimming in the tank and subsequent 5-min observation on a dry platform at room temperature. In cold water however, there was an observable difference between ADMS and WT rats. Toward the end of the 2-min swimming period, ADMS rats had difficulties maintaining axial orientation and

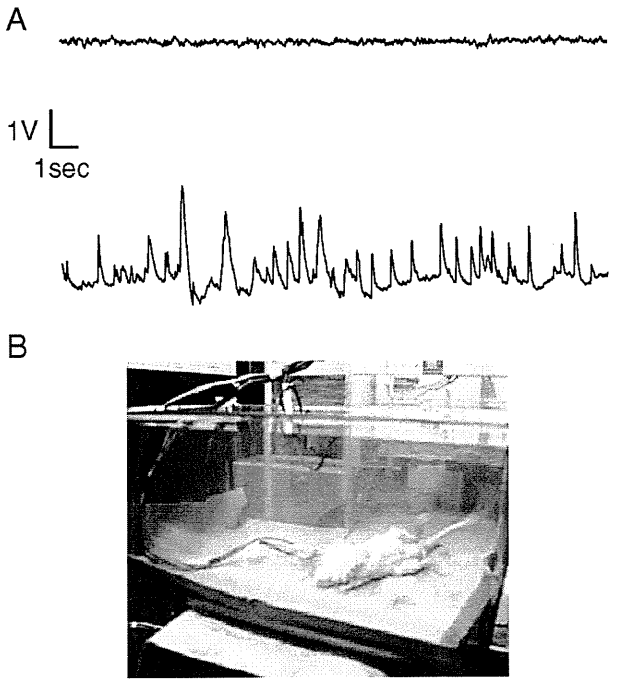

Fig. 5 – Cortical EEG recording in ADMS rat by cold-swim tests. (A) EEG recorded from an ADMS rat before the test (upper) and during the cold-swim induced clonus behaviour (lower). (B) A photograph shows characteristic posture during the clonus behaviour.

swimming, showing head shaking and twitching behaviour in the water. When removed from the water, ADMS rats exhibited severe neuromyotonia (Supplementary Video 4) and tremors, with the eyes shut and whiskers flickering. After a few minutes of tremors lasting, and even worsening, the rats demonstrated head nodding, forelimb clonus and rearing. Cortical EEG recordings showed aberrant spike-and-wave discharges (2-3 Hz) associated with clonus behaviours (Figs. 5A, B). The tremors and clonus phenotypes were reduced as time progressed, but when the animals started to walk, its movements were staggering and ataxic (Supplementary Video 5). Normal behaviour was fully recovered after 20 min. Cold-swim induced tremors, neuromyotonia, clonus, and motor incoordination, were present in all ADMS rats tested (n=7). In contrast, none of the behaviours was observed in WT rats (n=5).

2.7. *Electrophysiological properties of S309T channel*

To investigate the functional consequences of the S309T mutation on the Kv1.1 channel, we transfected HEK 293 cells with *Kcna1* cDNA (WT or S309T) and recorded whole-cell current responses. At a holding potential of −80 mV, current families were obtained by sequential 100-ms depolarizing commands from −100 to 50 mV, delivered in 10 mV increments. Typical delayed-rectifier potassium currents were recorded from cells expressing Kv1.1 WT, whereas minimal currents were detected from cells expressing Kv1.1 S309T or from mock-transfected cells (Figs. 6A, B). In western blot analysis, a single 56-kD band was detected in cells transfected with *Kcna1* WT or S309T cDNA (Fig. 6C). To investigate whether the S309T mutation has an effect on the intracellular trafficking of Kv1.1, we analysed the cell-surface expression of Kv1.1, by biotinylating the surface proteins on HEK cells. Precipitation of the solubilized biotinylated proteins with streptavidin beads, followed by western blotting, detected expression of both WT and S309T variants of Kv1.1 on the cell surface (Fig. 6D).

Because ADMS rats carrying the *Kcna1* S309T mutation dominantly display several neurological abnormalities, the opening of Kv1.1 channels may be disturbed when one or more S309T-containing subunits are incorporated into the tetrameric complex of Kv1.1 channels. To test this hypothesis, we co-injected cRNAs for WT and S309T mutant subunits in *Xenopus* oocytes, and measured current responses under a two electrode voltage clamp configuration. At a holding potential of −60 mV, current families were obtained by 500-ms depolarizing commands (with a 500 ms prepulse at −120 mV) from −60 to 60 mV, delivered in 20 mV increments. The co-injection of WT and S309T cRNA (1:1 ratio) resulted in reduced outward currents, with an approximately 80% smaller amplitude than that of WT-injected oocytes at 0 mV, suggesting a dominant-negative effect of the S309T subunit on the function of heterotetrameric Kv1.1 channels (Figs. 6E, F). Western blot analysis showed equivalent Kv1.1 protein expression levels among the three groups (WT, S309T and WT:S309T (1:1) co-injected) of oocytes (Fig. 6G).

3. Discussion

Table 1 summarizes the *Kcna1*-mutant animal models for EA1 previously reported in mice and rats. They exhibit diverse neurological phenotypes and show differing functional defects of the potassium channel, Kv1.1 (Herson et al., 2003; Petersson et al., 2003; Smart et al., 1998). *Kcna1*-knockout mice have a complete deletion of *Kcna1*, and have enormously contributed to our fundamental understanding of Kv1.1 function (Glasscock et al., 2010; Kopp-Scheinpflug et al., 2003; Lopantsev et al., 2003; Smart et al., 1998; Zhang et al., 1999; Zhou et al., 1998). Homozygous *Kcna1*-knockout mice exhibit various neurological defects, namely, spontaneous seizure activities associated with elevated excitability of the hippocampal CA3 neurons (Lopantsev et al., 2003), and/or of the auditory neurons of the medial nucleus of the trapezoid body (MNTB) (Kopp-Scheinpflug et al., 2003). Other defects include temperature-sensitive nerve excitability in the PNS (Zhou et al., 1998), alteration of GABAergic inhibition in cerebellar Purkinje cells (Zhang et al., 1999), and premature death potentially associated with cardiac dysfunction (Glasscock et al., 2010). However, to date, no mutation causing a complete deletion of the *KCNA1* gene has been reported in human EA1. Spontaneous mutant mice, *megencephaly*, expressing a truncated KCNA1 protein of 230 residues, recessively exhibit progressive brain overgrowth and epileptic behaviours similar to knockout mice (Persson et al., 2005; Petersson et al., 2003). *Kcna1*-knockin mice induced by the V408A EA1 mutation, show stress-induced loss of motor coordination, which mimics the symptoms of human EA1 (Herson et al., 2003). However, none of the mouse models shows spontaneous behavioural

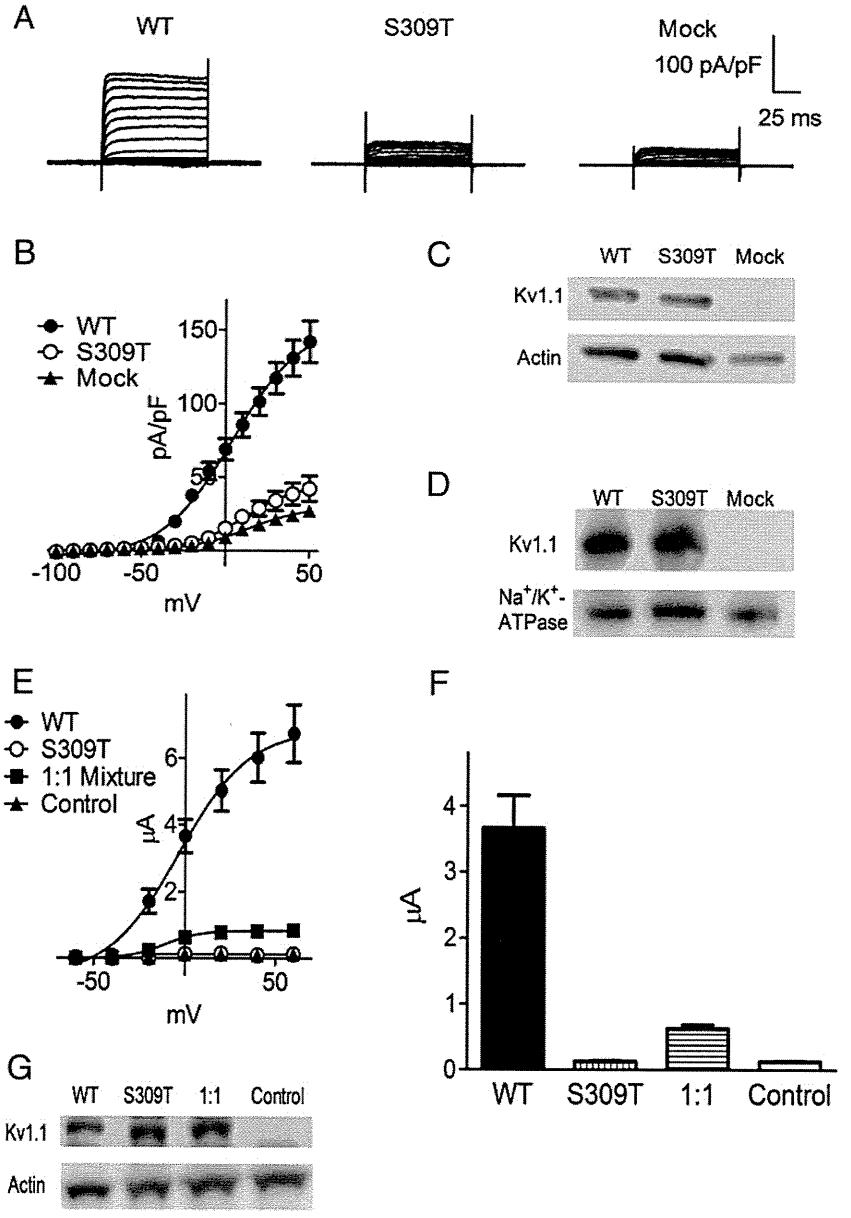

Fig. 6 – Electrophysiological properties of S309T channel. (A) Typical whole-cell current families recorded from HEK 293 cells transfected with cDNAs encoding Kv1.1 WT (left), S309T (centre) and transfection control (mock, right). Minimal currents were detected from cells expressing Kv1.1 S309T or from mock-transfected cells. (B) I–V relationships of Kv1.1 channels recorded from HEK cells transfected with each variant (n=4–5). (C, D) Western blot analysis of (C) whole cell lysate and (D) cell surface fractions of HEK cells transfected with each variant. Both WT and S309T Kv1.1 proteins were expressed on the cell surface. (E) I–V relationships of Kv1.1 channels recorded from *Xenopus* oocytes injected with WT cRNA, S309T cRNA and 1:1 mixture of WT and S309T cRNAs (n=4). The total amount of injected cRNAs was adjusted to 5 ng/oocyte. (F) Current amplitude recorded in response to 0 mV voltage pulse shown in (E). The co-injection of WT and S309T cRNA resulted in 80% smaller currents than WT-injected oocytes. (G) Western blot analysis indicated equivalent Kv1.1 protein expression levels among the three groups of cRNA injected oocytes, WT, S309T and WT:S309T (1:1) co-injected.

phenotypes in heterozygotes, in contrast to the ADMS rats, which we have shown to dominantly express convulsive seizures, myokymia and neuromyotonia. These neurological phenotypes are similar to symptoms of human EA1, and are severe compared with current mouse models. Interestingly, as far as we know, the myokymia phenotype detected by EMG recording in ADMS rats, has not been reported in any of the mouse models, but is always detected in individuals with human EA1. Considering EA1 patients exhibiting myokymia in the limbs or especially in the muscles of the face or the hands (Pessia and Hanna, 1993), myokymia with a predilection for forelimbs of ADMS rats may partially mimic the EA1 symptoms of human patients.

What mechanism is responsible for the phenotypic differences between the EA1 models? Strain-dependent genetic

Table 1 – Phenotype comparison of *Kcna1* mutant animals and relevance as EA1 models.

Animals	Mutation		Phenotypes				Protein functions in vitro		
			Lethality	Seizure (CNS)	Myokymia, neuromyotonia (PNS)	Episodic ataxia (cerebellum)	Channel activity	Expression, trafficking	Tetrameric channels
Kcna1 knockout mice (Smart et al., 1998)	Null	Hetero	–	± susceptible to flurothyl-induced seizures	–	–	↓↓↓ no activity	↓ half expression	–
		Homo	~50% die until 5 weeks	+++ spontaneous seizures start from 3–4 weeks	± cold-swim induced tremor and neuromyotonia	± cold-swim induced motor incoordination		↓↓↓ no expression	
megencephaly mice (Petersson et al., 2003)	Truncation at 230aa	Hetero	- (increased brain volume)	–	–	–	↓↓↓ no activity	–	Forming tetramers, impeded?
		Homo		+++ spontaneous seizures start from 5–6 weeks	+ startle responses	+ shakiness in gait		↓↓↓ trapped in endoplasmic reticulum	
V408A knockin mice (Herson et al., 2003)	Missense V408A	Hetero	–	–	–	± isoproterenol-induced motor incoordination	↓↓ reduced current, slow inactivation	Normal expression and trafficking	Interrupting WT-Kv1.1 channels
		Homo	embryonic lethal at E3-E9	–	–	–			
ADMS S309T rats	Missense S309T	Hetero	~80% die until 30 weeks	+++ spontaneous seizures start from 12–14 weeks	+++ myokymia, neuromyotonia, startle responses	± cold-swim induced motor incoordination	↓↓↓ no current	Normal expression and trafficking	Interrupting WT-Kv1.1 channels
		Homo	postnatal lethal at P10–P18	++++ spontaneous seizures start from P10	++++ extension of hind limbs, tremor	+++ ataxia			

background or species differences between mouse and rat likely play a part. Seizure onset was delayed or even prevented in F1 and BC1 progeny of BN rats, suggesting the influence of modifier gene(s). In human EA1, neuromyotonia is generally associated with KCNA1 mutations; conversely, epilepsy is not associated with mutations in potassium channels, but with other factors such as modifier genes (Pessia and Hanna, 1993; Poujois et al., 2006; Rajakulendran et al., 2007; Zuberi et al., 1999). In mice, impaired Ca^{2+}-channel function as a result of *Cacna1a* mutations, show improved seizure susceptibility by altering neuronal network excitability in *Kcna1*-knockout mice, demonstrating protective interactions between ion channel variants (Glasscock et al., 2007). A further interaction between *Kcna1* and another gene, *Lgi1*, was implicated in a rare autosomal dominant form of temporal lobe epilepsy, and shown to modulate fast inactivation of Kv1.1 (Schulte et al., 2006). Further genetic analysis focusing on seizure susceptibility in the (ADMS×BN)×BN backcross progeny may offer insights into the modifier gene(s) associated with seizure onset.

The distinct mutations of *Kcna1* may explain the wide variety of clinical phenotypes in EA1. Our expression studies of homomeric S309T Kv1.1 channels in HEK cells indicated cell-surface expression of the channels is non-functional in terms of their biophysical properties (Fig. 6). Heteromeric expression of S309T and WT Kv1.1 channels in *Xenopus* oocytes resulted in greatly reduced currents compared with WT Kv1.1 channels, suggesting the S309T mutation has a dominant-negative effect on the potassium channel, consistent with previous functional studies on EA1 mutations (Chen et al., 2007; D'Adamo et al., 1999; Imbrici et al., 2011; Zuberi et al., 1999). The *mceph* truncated protein, containing only the N-terminal domain, is retained in the endoplasmic reticulum and not expressed on the cell surface (Persson et al., 2005) (Table 1). On the other hand, V408A Kv1.1 channels show normal cell-surface expression and partially reduced potassium currents (Adelman et al., 1995). It was also reported that the V408A Kv1.1 channels reduce the rate of inactivation by a decreased affinity for the N-terminal inactivation domain of co-assembled WT Kv1.1 in heterotetramers, which could explain the dominant-negative effects of the V408A Kv1.1 channels (Imbrici et al., 2011). T226K Kv1.1 channels in EA1 also showed a dominant-negative effect when co-expressed in oocytes with the WT Kv1.1 (Chen et al., 2007). In addition, Kv1.1-containing channels in the mammalian central nervous system co-assembled with Kv1.2 and Kv1.4 subunits, which may be also interrupted by the cell-surface expressed mutated Kv1.1 subunit in heterotetramers (D'Adamo et al., 1999; Imbrici et al., 2006). The dominant-negative effects of the V408A Kv1.1 channels in knockin mice as well as S309T Kv1.1 channels in ADMS rats may explain the lethality of the homozygous animals, which are different from that of knockout and *mceph* mice.

In conclusion, using an ENU mutagenesis approach, we have generated *Kcna1*-mutant rats that dominantly express persistent myokymia, neuromyotonia, stress-induced motor incoordination and spontaneous convulsive seizures, as the first rat model of human EA1. The ADMS rat provides a useful animal model of human EA1 to understand the underlying mechanisms of the various clinical phenotypes of KCNA1-associated diseases.

4. Experimental procedures

4.1. *Rats and ENU mutagenesis*

Male F344/NSlc (F344) rats (Japan SLC, Hamamatsu, Japan) received two intraperitoneal (i.p.) injections of the chemical mutagen ENU (40 mg/kg) as previously described (Mashimo et al., 2008). Ten weeks after the second ENU injection, males were bred to untreated F344 females to generate ENU-mutagenized G1 progeny (mean mutation frequency: approximately 1 in 4 million base pairs). One female exhibiting muscle twitching and epileptic seizures, was identified and classified as an "affected" founder, then backcrossed to a F344 background, for ten generations (N2–N10), to remove latent ENU-induced mutations in other chromosomal regions. Heterozygous affected N10 males and females were intercrossed to generate the homozygous mutation.

The animal care and experimental procedures used were approved by the Animal Research Committee, Kyoto University and carried out according to the Regulation on Animal Experimentation at Kyoto University. The ADMS rat has been deposited into the National Bio Resource Project — Rat in Japan (NBPR-Rat No. 0458) and is available from the Project (http://www.anim.med.kyoto-u.ac.jp/nbr).

4.2. *Electromyography (EMG) recording*

Rats at 16 weeks of age were used for electromyography (EMG) recordings from muscles in the forelimb (musculus triceps brachii) and hindlimb (musculus quadriceps femoris). To implant EMG electrodes, rats were anesthetized with pentobarbital sodium (50 mg/kg i.p.). Enamel-coated stainless-steel electrodes (100 μm diameter), were prepared by flexing the electrode into a hair-pin curve, 5 mm from the distal end of the electrode. Electrodes were then hooked onto the bevel edge of a 23 gauge injection needle and inserted into the muscle through the overlying skin. The injection needle was removed, leaving the electrode implanted in the appropriate muscle. Pairs of electrodes were implanted in each muscle, to allow bipolar recording, and a ground electrode was inserted subcutaneously on the back. After recovery from anaesthesia, EMG activity was recorded under freely moving conditions, and combined with behavioural observations made using an amplifier (MEG-6108; Nihon Kohden, Tokyo, Japan) and a thermal alley recorder (RTA-1100; Nihon Kohden). The recorded signals were stored (PowerLab ML845; AD Instruments, Bella Vista, Australia) for analysis.

4.3. *Electroencephalogram (EEG) recording*

Rats at 10–20 weeks of age were anesthetized with pentobarbital sodium (50 mg/kg i.p.), and fixed in a stereotaxic instrument (David Kopf Instruments, Tujunga, USA) for implantation of EEG electrodes. Small holes were made in the skull, and screw electrodes were placed on the surface of the right frontal cortex. Enamel-coated stainless-steel electrodes were implanted in the hippocampus (3.8 mm caudal and 2.0 mm lateral to the bregma, and 2.2 mm from the cortex surface). A reference electrode was implanted on the left frontal cranium. The electrodes were then connected to a miniature plug and fixed to the skull with dental cement. After a 1-week recovery period, animals

with chronically implanted electrodes were placed in a shielded box (40×40×40 cm^3). Under freely moving conditions, continuous EEG recordings were made for 3 h during daytime (light-on), with behavioural observations made using an amplifier (MEG-6108; Nihon Kohden) and a thermal alley recorder (RTA-1100; Nihon Kohden). The recorded signals were stored (PowerLab ML845; AD Instruments) for analysis.

4.4. *Antiepileptic drug testing*

Carbamazepine (Sigma-Aldrich Co., St. Louis, USA) dissolved in polyethylene glycol 400 (PEG 400) was used for drug testing (20 mg/kg i.p.), or saline solution (1 ml/kg i.p.) as control. Five ADMS rats at 16–19 weeks of age were observed for 3 h during daytime (light-on) from 30 min after the administration.

4.5. *Histopathology*

Rats at 16–19 weeks of age were deeply anesthetized with sodium pentobarbital (50 mg/kg i.p.). Brains were removed, post-fixed in Bouin's fixative and paraffin embedded. 4 μm paraffin sections were cut and stained with haematoxylin and eosin to evaluate morphological changes.

4.6. *Genetic mapping of Adms*

We produced a total of 180 (BN/SsNSlc×ADMS)×BN/SsNSlc backcross progeny. Genotyping for the *Adms* locus was performed in rats that exhibited the twitching phenotype at 10–14 weeks of age, since spontaneous seizures were not observed in the backcross progeny until at least 20 weeks of age. To localize the *Adms* locus to a specific chromosomal region, we performed genome-wide scanning on DNA samples using a panel of 121 simple sequence length polymorphism (SSLP) markers that cover all the autosomal chromosomes (Chrs). Genomic DNA was prepared from tail biopsies using an automatic DNA purification system (PI-200; Kurabo, Osaka, Japan). All PCRs were performed for 35 cycles (denaturation at 94 °C for 30 s, annealing at 60 °C for 1 min, and extension at 72 °C for 45 s), using Taq polymerase (Takara Bio, Otsu, Japan). PCR products were examined on 4% agarose gels with ethidium bromide staining.

4.7. *Sequence analysis*

The primers used for sequencing the coding regions of *Kcna1*, *Kcna5*, and *Kcna6* are described in Supplementary Table 1. PCR products from genomic DNA were reacted with BigDye Terminator v3.1 cycle sequencing mix (Applied Biosystems, Foster City, USA), followed by the standard protocol for the Applied Biosystems 3100 DNA Sequencer.

4.8. *Western blotting*

Protein lysates were prepared from P10 rat brain as previously described (Imai et al., 2007). 25 μg of each sample was separated on 10% Bis–Tris polyacrylamide gels and analysed by western blotting using rat KCNA1 (ab32433; Abcam, Cambridge, UK) and β-actin (AC-40; Sigma Aldrich) primary antibodies. Secondary antibodies against rabbit IgG (NA934; GE Healthcare Bio-Sciences, Little Chalfont, UK) and mouse IgG (NA931; GE Healthcare Biosciences) were used, respectively.

4.9. *Swimming tests*

Rats at 5 weeks of age were placed in the middle of a tank (30 cm×60 cm, filled with water to a depth of 20 cm) to swim. The water temperature was 17 or 38 °C, and the swim time was 2 min. After swimming, the rats were placed on a dry platform (room temperature 24 °C) for behavioural observation.

4.10. *Cell culture and transfection*

Rat *Kcna1* is encoded by a single exon, allowing the coding region of wild-type (WT) or S309T mutant *Kcna1* to be PCR amplified from genomic DNA. PCR products were inserted into pGEM-T Easy (Promega, Fitchburg, USA) and sequenced to confirm the presence of the S309T mutation. The full length cDNA for each variant (*Kcna1* WT or S309T), was subcloned into pcDNA3.1(–) (Invitrogen, Carlsbad, USA), for western blot analysis, and pIRES2-EGFP (Clontech, Mountain View, USA) for current recording. mRNA was transcribed in vitro using T7-RNA polymerase and a High Yield Capped RNA transcription kit (EPICENTRE Biotechnologies, Madison, USA).

Human embryonic kidney (HEK) 293 cells were grown to 80% confluence in Dulbecco's modified Eagle's medium supplemented with 10% foetal bovine serum, 50 U/ml penicillin and 50 μg/ml streptomycin at 37 °C. Cells were transfected with Lipofectamine 2000 (Invitrogen). For western blot analysis, cells were transfected with pcDNA3.1(–) containing *Kcna1* WT or S309T cDNAs, and maintained for 24 h before harvesting. For whole-cell current recording, cells were transfected with pIRES2-EGFP containing *Kcna1* WT or S309T cDNAs, then plated on glass coverslips at 10% confluence 24 h after transfection, and maintained for another 24 h.

4.11. *Cell-surface biotinylation*

24 h after transfection, HEK 293 cells in 35 mm tissue culture dishes were washed with PBS-CM (PBS containing 1 mM $MgCl_2$ and 0.1 mM $CaCl_2$), then incubated in 0.8 ml of EZ-Link Sulfo-NHS-biotin solution (1 mg/ml in PBS-CM; Thermo Scientific, Waltham, USA) for 30 min on ice. After washing with ice-cold quenching solution (PBS-CM containing 100 mM glycine), cells were incubated in 1 mL quenching solution for 45 min at 4 °C before harvesting, followed by centrifugation for 6 min at 6000×*g*. Cells were then solubilized on ice in 300 μl RIPA buffer (1% Triton X-100, 0.1% SDS, 150 mM NaCl, 1 mM EDTA and 50 mM Tris, pH 7.5 with HCl) containing 1% protease inhibitor cocktail (Invitrogen). The resulting cell lysate was centrifuged for 20 min at 14000×*g*, and the supernatant collected. UltraLink® immobilized streptavidin (Thermo Scientific) was added to the supernatant at a ratio of 1:6, and then incubated overnight at 4 °C with agitation. Next, samples were centrifuged for 1 min at 5000×*g*, and the resin washed with RIPA buffer, high-salt buffer (0.1% Triton X-100, 500 mM NaCl, 5 mM EDTA, 50 mM Tris, pH 7.4 with HCl), and 50 mM Tris (pH7.4 with HCl). Proteins were eluted from the resin by the addition of LDS sample buffer (Invitrogen).

4.12. *Electrophysiological recording from HEK 293 cells*

Whole-cell currents were recorded at room temperature with an EPC 9 amplifier (HEKA, Lambrecht, Germany). Currents were sampled and analysed with Patchmaster 2.43 software (HEKA). Patch pipettes were made from borosilicate glass capillaries (1.5-mm outer diameter; Narishige, Tokyo, Japan) using a P-87 micropipette puller (Sutter Instruments, Novato, USA). The resistance ranged from 2 to 4 MΩ when filled with pipette solution (138 mM NaCl, 5.4 mM KCl, 1.2 mM $MgCl_2$, 1 mM $CaCl_2$, 10 mM EGTA, 10 mM HEPES, 10 mM glucose, pH 7.3 with NaOH). The recording solution was 138 mM NaCl, 5.4 mM KCl, 1.2 mM $MgCl_2$, 1 mM $CaCl_2$, 10 mM EGTA, 10 mM HEPES, 10 mM glucose, pH 7.3 with NaOH.

4.13. *Electrophysiological recording from* ***Xenopus*** *oocytes*

Small pieces of ovary were isolated from cold-anesthetized *Xenopus laevis* and incubated in Ca^{2+}-free solution (88 mM NaCl, 1 mM KCl, 0.82 mM $MgSO_4$, 2.4 mM $NaHCO_3$, 7.5 mM Tris, pH 7.4 with HCl), containing 1.5 mg/ml collagenase (Sigma-Aldrich) at 20 °C for 3 h. Stage V and VI oocytes were selected and injected with 25 nl of cRNA solution for each *Kcna1* variant (WT or S309T). The injected oocytes were maintained at 20 °C for 4 days in modified Barth's solution (88 mM NaCl, 1 mM KCl, 0.41 mM $CaCl_2$, 0.33 mM $Ca(NO_3)_2$, 0.82 mM $MgSO_4$, 2.4 mM $NaHCO_3$, 7.5 mM Tris, pH7.4 with HCl), supplemented with 300 μg/ml sodium pyruvate, 10 U/ml penicillin and 10 μg/ml streptomycin. Currents were recorded at 20 °C with an OC-725C amplifier (Warner Instruments, Hamden, USA). Currents were sampled and analysed with a PowerLab 2/25 system (AD Instruments) and Scope 4.0.7 software (AD Instruments). The injected oocytes were voltage-clamped at a holding potential of −60 mV with two intracellular glass electrodes (1–2 MΩ with 3 M KCl), made from borosilicate glass capillaries (1.5-mm outer diameter; Narishige) using a PE-2 puller (Narishige). The recording solution was 115 mM NaCl, 2 mM KCl, 2 mM $CaCl_2$, 2 mM $MgCl_2$, 10 mM HEPES, pH 7.2 with NaOH.

Supplementary materials related to this article can be found online at doi:10.1016/j.brainres.2011.11.023.

Acknowledgments

This work was supported in part by Grant-in-Aid for Scientific Research from the Ministry of Education, Culture, Sports, Science and Technology (16200029 to T.M.); and Industrial Technology Research Grant Program from the New Energy and Industrial Technology Development Organization of Japan (08A02004a to T.M.). We would like to thank Fumi Tagami and Yayoi Kunihiro for technical help, and Masashi Sasa for his helpful consultations.

REFERENCES

Adelman, J.P., Bond, C.T., Pessia, M., Maylie, J., 1995. Episodic ataxia results from voltage-dependent potassium channels with altered functions. Neuron 15, 1449–1454.

Bretschneider, F., Wrisch, A., Lehmann-Horn, F., Grissmer, S., 1999. Expression in mammalian cells and electrophysiological characterization of two mutant Kv1.1 channels causing episodic ataxia type 1 (EA-1). Eur. J. Neurosci. 11, 2403–2412.

Browne, D.L., Gancher, S.T., Nutt, J.G., Brunt, E.R., Smith, E.A., Kramer, P., Litt, M., 1994. Episodic ataxia/myokymia syndrome is associated with point mutations in the human potassium channel gene, KCNA1. Nat. Genet. 8, 136–140.

Browne, D.L., Brunt, E.R., Griggs, R.C., Nutt, J.G., Gancher, S.T., Smith, E.A., Litt, M., 1995. Identification of two new KCNA1 mutations in episodic ataxia/myokymia families. Hum. Mol. Genet. 4, 1671–1672.

Chen, H., von Hehn, C., Kaczmarek, L.K., Ment, L.R., Pober, B.R., Hisama, F.M., 2007. Functional analysis of a novel potassium channel (KCNA1) mutation in hereditary myokymia. Neurogenetics 8, 131–135.

Comu, S., Giuliani, M., Narayanan, V., 1996. Episodic ataxia and myokymia syndrome: a new mutation of potassium channel gene Kv1.1. Ann. Neurol. 40, 684–687.

D'Adamo, M.C., Imbrici, P., Sponcichetti, F., Pessia, M., 1999. Mutations in the KCNA1 gene associated with episodic ataxia type-1 syndrome impair heteromeric voltage-gated K(+) channel function. FASEB J. 13, 1335–1345.

Demos, M.K., Macri, V., Farrell, K., Nelson, T.N., Chapman, K., Accili, E., Armstrong, L., 2009. A novel KCNA1 mutation associated with global delay and persistent cerebellar dysfunction. Mov. Disord. 24, 778–782.

Eunson, L.H., Rea, R., Zuberi, S.M., Youroukos, S., Panayiotopoulos, C.P., Liguori, R., Avoni, P., McWilliam, R.C., Stephenson, J.B., Hanna, M.G., Kullmann, D.M., Spauschus, A., 2000. Clinical, genetic, and expression studies of mutations in the potassium channel gene KCNA1 reveal new phenotypic variability. Ann. Neurol. 48, 647–656.

Gilbert, G.J., Graves, T.D., Kullmann, D.M., 2011. Nongenetic factors influence severity of episodic ataxia type 1 in monozygotic twins. Neurology 76, 490 (author reply 490).

Glasscock, E., Qian, J., Yoo, J.W., Noebels, J.L., 2007. Masking epilepsy by combining two epilepsy genes. Nat. Neurosci. 10, 1554–1558.

Glasscock, E., Yoo, J.W., Chen, T.T., Klassen, T.L., Noebels, J.L., 2010. Kv1.1 potassium channel deficiency reveals brain-driven cardiac dysfunction as a candidate mechanism for sudden unexplained death in epilepsy. J. Neurosci. 30, 5167–5175.

Glaudemans, B., van der Wijst, J., Scola, R.H., Lorenzoni, P.J., Heister, A., van der Kemp, A.W., Knoers, N.V., Hoenderop, J.G., Bindels, R.J., 2009a. A missense mutation in the Kv1.1 voltage-gated potassium channel-encoding gene KCNA1 is linked to human autosomal dominant hypomagnesemia. J. Clin. Invest. 119, 936–942.

Glaudemans, B., van der Wijst, J., Scola, R.H., Lorenzoni, P.J., Heister, A., van der Kemp, A.W., Knoers, N.V., Hoenderop, J.G., Bindels, R.J., 2009b. A missense mutation in the Kv1.1 voltage-gated potassium channel-encoding gene KCNA1 is linked to human autosomal dominant hypomagnesemia. J. Clin. Invest. 119, 936–942.

Graves, T.D., Rajakulendran, S., Zuberi, S.M., Morris, H.R., Schorge, S., Hanna, M.G., Kullmann, D.M., 2010. Nongenetic factors influence severity of episodic ataxia type 1 in monozygotic twins. Neurology 75, 367–372.

Herson, P.S., Virk, M., Rustay, N.R., Bond, C.T., Crabbe, J.C., Adelman, J.P., Maylie, J., 2003. A mouse model of episodic ataxia type-1. Nat. Neurosci. 6, 378–383.

Imai, Y., Inoue, H., Kataoka, A., Hua-Qin, W., Masuda, M., Ikeda, T., Tsukita, K., Soda, M., Kodama, T., Fuwa, T., Honda, Y., Kaneko, S., Matsumoto, S., Wakamatsu, K., Ito, S., Miura, M., Aosaki, T., Itohara, S., Takahashi, R., 2007. Pael receptor is involved in dopamine metabolism in the nigrostriatal system. Neurosci. Res. 59, 413–425.

Imbrici, P., D'Adamo, M.C., Kullmann, D.M., Pessia, M., 2006. Episodic ataxia type 1 mutations in the KCNA1 gene impair the fast inactivation properties of the human potassium channels

Kv1.4-1.1/Kvbeta1.1 and Kv1.4-1.1/Kvbeta1.2. Eur. J. Neurosci. 24, 3073–3083.
Imbrici, P., Gualandi, F., D'Adamo, M.C., Masieri, M.T., Cudia, P., De Grandis, D., Mannucci, R., Nicoletti, I., Tucker, S.J., Ferlini, A., Pessia, M., 2008. A novel KCNA1 mutation identified in an Italian family affected by episodic ataxia type 1. Neuroscience 157, 577–587.
Imbrici, P., D'Adamo, M.C., Grottesi, A., Biscarini, A., Pessia, M., 2011. Episodic ataxia type 1 mutations affect fast inactivation of K^+ channels by a reduction in either subunit surface expression or affinity for inactivation domain. Am. J. Physiol. Cell Physiol. 300, C1314–C1322.
Johnston, J., Forsythe, I.D., Kopp-Scheinpflug, C., 2010. Going native: voltage-gated potassium channels controlling neuronal excitability. J. Physiol. 588, 3187–3200.
Kinali, M., Jungbluth, H., Eunson, L.H., Sewry, C.A., Manzur, A.Y., Mercuri, E., Hanna, M.G., Muntoni, F., 2004. Expanding the phenotype of potassium channelopathy: severe neuromyotonia and skeletal deformities without prominent Episodic Ataxia. Neuromuscul. Disord. 14, 689–693.
Klein, A., Boltshauser, E., Jen, J., Baloh, R.W., 2004. Episodic ataxia type 1 with distal weakness: a novel manifestation of a potassium channelopathy. Neuropediatrics 35, 147–149.
Knight, M.A., Storey, E., McKinlay Gardner, R.J., Hand, P., Forrest, S.M., 2000. Identification of a novel missense mutation L329I in the episodic ataxia type 1 gene KCNA1—a challenging problem. Hum. Mutat. 16, 374.
Kopp-Scheinpflug, C., Fuchs, K., Lippe, W.R., Tempel, B.L., Rubsamen, R., 2003. Decreased temporal precision of auditory signaling in Kcna1-null mice: an electrophysiological study in vivo. J. Neurosci. 23, 9199–9207.
Lee, H., Wang, H., Jen, J.C., Sabatti, C., Baloh, R.W., Nelson, S.F., 2004. A novel mutation in KCNA1 causes episodic ataxia without myokymia. Hum. Mutat. 24, 536.
Lopantsev, V., Tempel, B.L., Schwartzkroin, P.A., 2003. Hyperexcitability of CA3 pyramidal cells in mice lacking the potassium channel subunit Kv1.1. Epilepsia 44, 1506–1512.
Mashimo, T., Yanagihara, K., Tokuda, S., Voigt, B., Takizawa, A., Nakajima, R., Kato, M., Hirabayashi, M., Kuramoto, T., Serikawa, T., 2008. An ENU-induced mutant archive for gene targeting in rats. Nat. Genet. 40, 514–515.
Mashimo, T., Ohmori, I., Ouchida, M., Ohno, Y., Tsurumi, T., Miki, T., Wakamori, M., Ishihara, S., Yoshida, T., Takizawa, A., Kato, M., Hirabayashi, M., Sasa, M., Mori, Y., Serikawa, T., 2010. A missense mutation of the gene encoding voltage-dependent sodium channel (Nav1.1) confers susceptibility to febrile seizures in rats. J. Neurosci. 30, 5744–5753.
Persson, A.S., Klement, G., Almgren, M., Sahlholm, K., Nilsson, J., Petersson, S., Arhem, P., Schalling, M., Lavebratt, C., 2005. A truncated Kv1.1 protein in the brain of the megencephaly mouse: expression and interaction. BMC Neurosci. 6, 65.
Pessia, M., Hanna, M.G., 1993. Episodic Ataxia Type 1. Vol. In: Pagon, R.A., Bird, T.D., Dolan, C.R., Stephens, K. (Eds.), GeneReviews. University of Washington, Seattle, Seattle WA (Vol.).
Petersson, S., Persson, A.S., Johansen, J.E., Ingvar, M., Nilsson, J., Klement, G., Arhem, P., Schalling, M., Lavebratt, C., 2003. Truncation of the Shaker-like voltage-gated potassium channel, Kv1.1, causes megencephaly. Eur. J. Neurosci. 18, 3231–3240.
Poujois, A., Antoine, J.C., Combes, A., Touraine, R.L., 2006. Chronic neuromyotonia as a phenotypic variation associated with a new mutation in the KCNA1 gene. J. Neurol. 253, 957–959.
Rajakulendran, S., Schorge, S., Kullmann, D.M., Hanna, M.G., 2007. Episodic ataxia type 1: a neuronal potassium channelopathy. Neurotherapeutics 4, 258–266.
Rho, J.M., Szot, P., Tempel, B.L., Schwartzkroin, P.A., 1999. Developmental seizure susceptibility of kv1.1 potassium channel knockout mice. Dev. Neurosci. 21, 320–327.
Scheffer, H., Brunt, E.R., Mol, G.J., van der Vlies, P., Stulp, R.P., Verlind, E., Mantel, G., Averyanov, Y.N., Hofstra, R.M., Buys, C.H., 1998. Three novel KCNA1 mutations in episodic ataxia type I families. Hum. Genet. 102, 464–466.
Schulte, U., Thumfart, J.O., Klocker, N., Sailer, C.A., Bildl, W., Biniossek, M., Dehn, D., Deller, T., Eble, S., Abbass, K., Wangler, T., Knaus, H.G., Fakler, B., 2006. The epilepsy-linked Lgi1 protein assembles into presynaptic Kv1 channels and inhibits inactivation by Kvbeta1. Neuron 49, 697–706.
Shook, S.J., Mamsa, H., Jen, J.C., Baloh, R.W., Zhou, L., 2008. Novel mutation in KCNA1 causes episodic ataxia with paroxysmal dyspnea. Muscle Nerve 37, 399–402.
Smart, S.L., Lopantsev, V., Zhang, C.L., Robbins, C.A., Wang, H., Chiu, S.Y., Schwartzkroin, P.A., Messing, A., Tempel, B.L., 1998. Deletion of the K(V)1.1 potassium channel causes epilepsy in mice. Neuron 20, 809–819.
Tomlinson, S.E., Tan, S.V., Kullmann, D.M., Griggs, R.C., Burke, D., Hanna, M.G., Bostock, H., 2010. Nerve excitability studies characterize Kv1.1 fast potassium channel dysfunction in patients with episodic ataxia type 1. Brain 133, 3530–3540.
Wenzel, H.J., Vacher, H., Clark, E., Trimmer, J.S., Lee, A.L., Sapolsky, R.M., Tempel, B.L., Schwartzkroin, P.A., 2007. Structural consequences of Kcna1 gene deletion and transfer in the mouse hippocampus. Epilepsia 48, 2023–2046.
Wulff, H., Castle, N.A., Pardo, L.A., 2009. Voltage-gated potassium channels as therapeutic targets. Nat. Rev. Drug Discov. 8, 982–1001.
Yoshimi, K., Tanaka, T., Takizawa, A., Kato, M., Hirabayashi, M., Mashimo, T., Serikawa, T., Kuramoto, T., 2009. Enhanced colitis-associated colon carcinogenesis in a novel Apc mutant rat. Cancer Sci. 100, 2022–2027.
Zerr, P., Adelman, J.P., Maylie, J., 1998. Characterization of three episodic ataxia mutations in the human Kv1.1 potassium channel. FEBS Lett. 431, 461–464.
Zhang, C.L., Messing, A., Chiu, S.Y., 1999. Specific alteration of spontaneous GABAergic inhibition in cerebellar purkinje cells in mice lacking the potassium channel Kv1. 1. J. Neurosci. 19, 2852–2864.
Zhou, L., Zhang, C.L., Messing, A., Chiu, S.Y., 1998. Temperature-sensitive neuromuscular transmission in Kv1.1 null mice: role of potassium channels under the myelin sheath in young nerves. J. Neurosci. 18, 7200–7215.
Zuberi, S.M., Eunson, L.H., Spauschus, A., De Silva, R., Tolmie, J., Wood, N.W., McWilliam, R.C., Stephenson, J.B., Kullmann, D.M., Hanna, M.G., 1999. A novel mutation in the human voltage-gated potassium channel gene (Kv1.1) associates with episodic ataxia type 1 and sometimes with partial epilepsy. Brain 122 (Pt 5), 817–825.

Epilepsia, 52(5):1010–1017, 2011
doi: 10.1111/j.1528-1167.2011.03046.x

FULL-LENGTH ORIGINAL RESEARCH

Therapy for hyperthermia-induced seizures in *Scn1a* mutant rats

***Keiichiro Hayashi, †Satoshi Ueshima, ‡Mamoru Ouchida, §Tomoji Mashimo, *Teiichi Nishiki, †Toshiaki Sendo, §Tadao Serikawa, *Hideki Matsui, and *Iori Ohmori**

*Department of Physiology, Graduate School of Medicine, Dentistry, and Pharmaceutical Sciences, Okayama University, Okayama, Japan; †Department of Pharmacy, Okayama University Hospital, Okayama, Japan; ‡Department of Molecular Genetics, Graduate School of Medicine, Dentistry, and Pharmaceutical Sciences, Okayama University, Okayama, Japan; and §Institute of Laboratory Animals, Graduate School of Medicine, Kyoto University, Kyoto, Japan

Summary

Purpose: Mutations in the *SCN1A* gene, which encodes the α1 subunit of voltage-gated sodium channels, cause generalized epilepsy with febrile seizures plus (GEFS+) and severe myoclonic epilepsy of infancy (SMEI). N1417H-*Scn1a* mutant rats are considered to be an animal model of human FS+ or GEFS+. To assess the pharmacologic validity of this model, we compared the efficacies of eight different antiepileptic drugs (AEDs) for the treatment of hyperthermia-induced seizures using N1417H-*Scn1a* mutant rats.

Methods: AEDs used in this study included valproate, carbamazepine (CBZ), phenobarbital, gabapentin, acetazolamide, diazepam (DZP), topiramate, and potassium bromide (KBr). The effects of these AEDs were evaluated using the hot water model, which is a model of experimental FS. Five-week-old rats were pretreated with each AED and immersed in water at 45°C to induce hyperthermia-induced seizures. The seizure manifestations and video-electroencephalographic recordings were evaluated. Furthermore, the effects of each AED on motor coordination and balance were assessed using the balance-beam test.

Key Findings: KBr significantly reduced seizure durations, and its anticonvulsant effects were comparable to those of DZP. On the other hand, CBZ decreased the seizure threshold. In addition, DZP and not KBr showed significant impairment in motor coordination and balance.

Significance: DZP and KBr showed potent inhibitory effects against hyperthermia-induced seizures in the *Scn1a* mutant rats, whereas CBZ exhibited adverse effects. These responses to hyperthermia-induced seizures were similar to those in patients with GEFS+ and SMEI. N1417H-*Scn1a* mutant rats may, therefore, be useful for testing the efficacy of new AEDs against FS in GEFS+ and SMEI patients.

KEY WORDS: Febrile seizure, Animal models, *Scn1a* gene, Generalized epilepsy with febrile seizures plus, Severe myoclonic epilepsy of infancy.

Febrile seizures (FS) are the most common convulsive disorder and affect 2–5% of children between the ages of 6 months and 6 years (Verity et al., 1985; Hauser, 1994; Offringa & Moyer, 2001). Although most FS are benign, known as simple FS, and do not require treatment, 2–7% of patients with FS subsequently develop epilepsy (Baulac et al., 2004). Generalized epilepsy with febrile seizures plus (GEFS+) is a familial epileptic syndrome characterized by FS persisting beyond 6 years and subsequent development of various types of epilepsy, including generalized tonic–clonic, myoclonic, and absence seizures (Scheffer & Berkovic, 1997). In severe myoclonic epilepsy of infancy (SMEI; also known as Dravet syndrome), repetitive FS begin in the first year of life, and life-threatening status epilepticus is often provoked by fever. Therefore, appropriate treatment of FS is important for patients with GEFS+ and SMEI.

Heterozygous mutations in *SCN1A*, a gene encoding the α1 subunit in voltage-gated sodium channels ($Na_V1.1$), are responsible for GEFS+ and SMEI. Mutations in *SCN1A* account for 80% of SMEI cases and 10% of GEFS+ cases (Claes et al., 2001; Ohmori et al., 2002; Hattori et al., 2008). Developments in genetic engineering have enabled the generation of various genetically modified animals, and many researchers can now investigate pathology and new disease treatments using these animals.

Recently, Mashimo et al. generated *Scn1a* mutant rats (F344/NSlc-*Scn1a*^{Kyo811}) with the missense mutation,

Accepted February 1, 2011; Early View publication April 11, 2011.
Address correspondence to Iori Ohmori, Department of Physiology, Graduate School of Medicine, Dentistry, and Pharmaceutical Sciences, Okayama University, 5-1 Shikata-cho, 2-chome, Okayama 700-8558, Japan. E-mail: iori@md.okayama-u.ac.jp

N1417H, using ENU mutagenesis (Mashimo et al., 2008, 2010). These N1417H-*Scn1a* mutant rats are considered an animal model of human FS+ or GEFS+. Generally, animal models of human diseases are required to fulfill three criteria, namely face validity, construct validity, and predictive validity (Chadman et al., 2009). Face validity incorporates a conceptual analogy to the symptoms of the human disease. Homozygous N1417H-*Scn1a* mutant rats exhibited susceptibility to hyperthermia-induced seizures, and their seizures persisted over the age of 5 weeks, whereas wild-type rats were unaffected. (Mashimo et al., 2010). Therefore, this model rat showed febrile seizures similar to those seen in patients with GEFS+ and SMEI. Second, construct validity incorporates a conceptual analogy to the cause of the human disease. These rats have an N1417H missense mutation in the causative *SCN1A* gene of GEFS+ and SMEI. N1417H was not detected in human patients, but the electrophysiologic properties of N1417H share a common molecular basis with most of SMEI, and some GEFS+ patients. Namely, the recombinant N1417H-human *SCN1A* mutation was revealed to have a loss-of-function effect on $Na_v1.1$, and the hippocampal neurons of these rats demonstrated impaired biophysical properties of inhibitory γ-aminobutyric acid (GABA)ergic neurons (Mashimo et al., 2010). We have confirmed that N1417H-*Scn1a* mutant rats fulfilled these two criteria in our previous study. Herein, we addressed the third criterion: predictive validity. It incorporates the specificity of responses to treatments that are effective in the human disease. We herein evaluated the efficacy of antiepileptic drugs (AEDs) on hyperthermia-induced seizures in the model rats. Potassium bromide (KBr), a traditionally prescribed AED, was found to be as effective as diazepam (DZP), whereas carbamazepine (CBZ) showed adverse effects. These drug-mediated responses to hyperthermia-induced seizures in the new model rats were similar to those in patients with GEFS+ or SMEI.

Materials and Methods

Animals

Male homozygous N1417H-*Scn1a* mutant rats (F344/NSlc-*Scn1a*^{Kyo811}) (National Bio Resource Project for the Rat in Japan, Kyoto University, Kyoto, Japan) were used to assess the effects of AEDs against hyperthermia-induced seizures. The susceptibility of wild-type rats to hyperthermia decreases with age, and, therefore, these 5-week-old rats showed no indications of hyperthermia-induced seizures, whereas the homozygous N1417H-*Scn1a* mutant rats demonstrated generalized tonic–clonic seizures induced by hyperthermia until at least 10 weeks of age (Mashimo et al., 2010). The rats were maintained under standard laboratory conditions with a 12-h light/dark cycle and food and water ad libitum. All experiments were performed in accordance with protocols approved by the Institutional Animal Care and Use Committee of Okayama University.

Induction of hyperthermia-induced seizures

Experimental FS have been extensively studied in a well-established model in which FS are evoked by exposing the rat pups (postnatal day 8–15) to heated air (Holtzman et al., 1981; Schuchmann et al., 2006), hot water jet on the heads (Ullal et al., 1996), or hot water bathing (Klauenberg & Sparber, 1984). We used hot water bathing from the view point of animal welfare: namely, heated air requires longer exposure of the rats to hyperthermic environment and induces more severe seizures compared with hot water bathing (Fig. S1). Induction of hyperthermia-induced seizures was performed as described previously, with slight modifications (Mashimo et al., 2010). Hyperthermia was induced by placing the rats in a 19.0 × 24.7 × 15.5 cm water bath (Thermo minder SD mini, Taitec, Japan) filled with water at 45°C to a depth of 6 cm (Fig. 1A). The rats were kept in the water for a maximum of 5 min or until a seizure occurred. We confirmed that immersing the rats in 37 and 40°C water for 5 min did not evoke seizures (Fig. S2). When a seizure occurred, the rats were removed immediately from the bath and monitored until they recovered. Rectal temperature of the rats was measured immediately after seizure onset using a digital thermometer (BDT-100; Bioresearch Center, Aichi, Japan) connected to a rectal probe (Ret-2; Physitemp, Clifton, NJ, U.S.A.). Each rat was assigned a score based on the most severe seizure observed. The seizure parameters were scored as follows: (0) no response; (1) head nodding with brief twitching movements (Fig. 1B); (2) repetitive myoclonic jerks with postural tone (Fig. 1C); (3) jumping and/or running fits (Fig. 1D); (4) generalized tonic–clonic seizure with loss of postural tone (Fig. 1E); and (5) death due to continuous convulsions. Seizure parameters were scored by an investigator who was blinded to the treatment received. All procedures were recorded using a video camera.

Treatment with AEDs

To assess the pharmacologic validation of N1417H-*Scn1a* mutant rats, AEDs that have been established to be effective in patients with GEFS+ and SMEI were chosen. AEDs used in the present study included sodium valproate (VPA-Na; Sigma-Aldrich, Tokyo, Japan), phenobarbital sodium (PB-Na; Wako, Osaka, Japan), diazepam (DZP; Wako), carbamazepine (CBZ; Sigma-Aldrich), acetazolamide sodium (AZA-Na, Diamox; Sanwa, Aichi, Japan), potassium bromide (KBr; Wako), topiramate (TPM; Toronto Research Chemicals, Toronto, ON, Canada), and gabapentin (GBP; Toronto Research Chemicals). VPA-Na, PB-Na, AZA-Na, KBr, and GBP were dissolved in saline. CBZ, DZP, and TPM were suspended in 10% polyethylene glycol 400 with saline. The rats were fasted overnight and orally administered each AED. Experimental conditions were determined based on the results of preliminary studies (Fig. S3). Because the appropriate range of each AED for the model rats is not known, we referred to the doses used to treat human epilepsy. The therapeutic range of each AED was

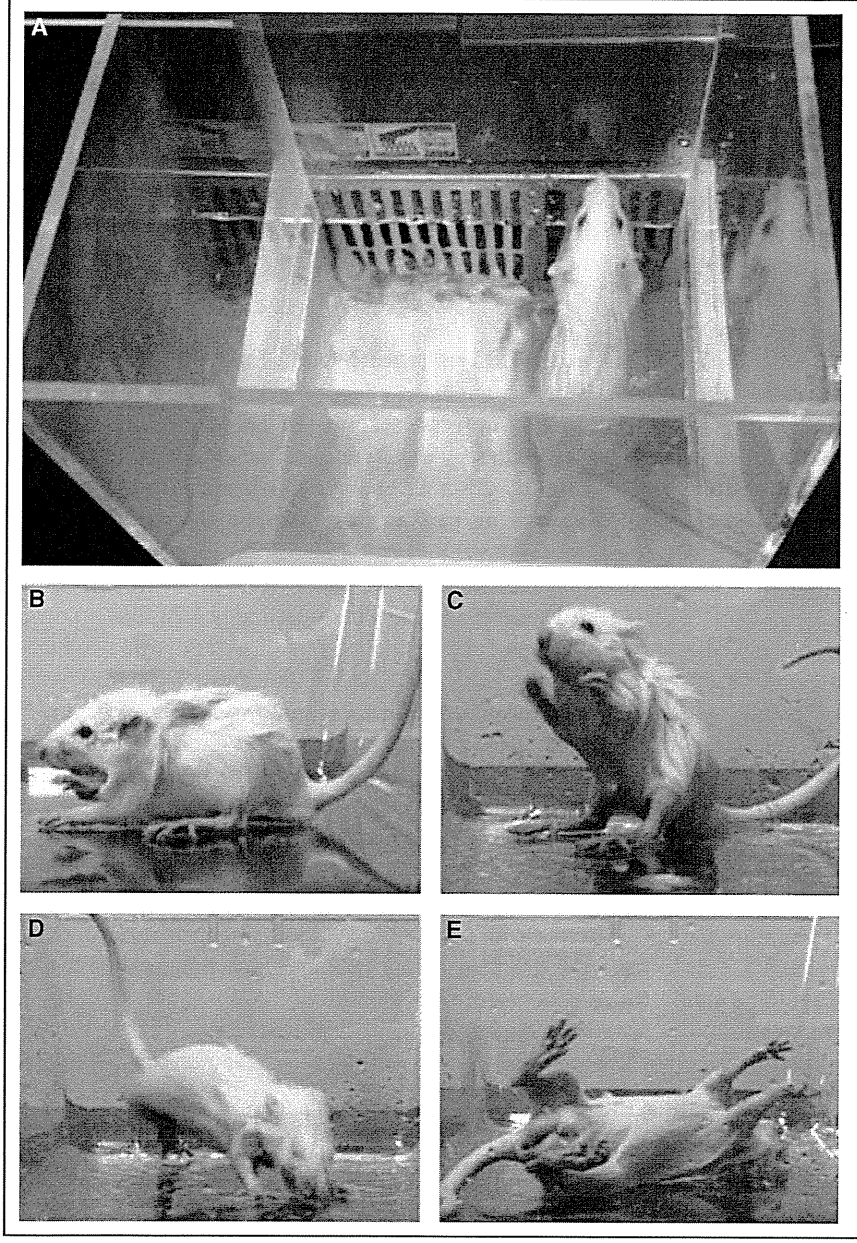

Figure 1.
Hyperthermia-induced seizures in *Scn1a* mutant rats. (**A**) Hyperthermia was induced by placing the rats in a water bath filled with water at 45°C. (**B**) Head nodding and brief twitching movements were classified as a score of 1. (**C**) Repetitive myoclonic jerks of the forelimbs with a postural tone were classified as a score of 2. (**D**) Jumping and/or running fits were classified as a score of 3. (**E**) Generalized tonic–clonic seizures with loss of postural tone were classified as a score of 4. *Epilepsia* © ILAE

determined according to previous literature as follows; VPA, 40–120 μg/ml (Schmidt, 2009); CBZ, 4–12 μg/ml (Eadie, 2001); PB, 10–40 μg/ml (Schmidt, 2009); GBP, 2–20 μg/ml (McLean, 1999); AZA, 10–20 μg/ml (Granero et al., 2007); DZP, 0.2–0.6 μg/ml (Ogutu et al., 2002); and KBr, 500–1,500 μg/ml (Ryan & Baumann, 1999). In cases where the blood concentration did not reach the therapeutic range, a higher dose was administrated to achieve a concentration higher than the top of the therapeutic range of each AED. Seizures were induced when the blood concentration of each AED elevated to an adequate level. VPA-Na (200 mg/kg) was administered for 30 min; CBZ (200 mg/kg), 120 min; PB-Na (50 mg/kg), 240 min; GBP (100 mg/kg), 90 min; AZA-Na (55 mg/kg), 30 min; DZP (5 mg/kg), 15 min; TPM (80 mg/kg), 90 min; and KBr (1,800 mg/kg), 90 min before seizures were induced. Experimental conditions of DZP and TPM administration were determined based on previous studies (Ishihara et al., 2000; Borowicz et al., 2003; Sendrowski et al., 2007). The temperature threshold was measured using the rectal temperature of the rats immediately after seizure onset, in addition to the duration of the seizure and the seizure severity score. After seizure termination, blood samples were obtained from the tail vein of the rats, and the blood concentration of each AED was then measured. Measurement of the blood concentrations of each AED was performed as described in Data S1.

Electroencephalography

Ictal electroencephalography (EEG) patterns were also analyzed for four AEDs (AZA, TPM, DZP, and KBr), which

exhibit remarkable therapeutic effects and CBZ, which may aggravate hyperthermia-induced seizures. At 4 weeks of age, the rats were implanted with electrodes for EEG recordings. Under pentobarbital sodium anesthesia (35 mg/kg, i.p., Nembutal; Abbott Laboratories, Abbott Park, IL, U.S.A.), the rats were fixed to a stereotaxic apparatus (SR-5M; Narishige, Tokyo, Japan). Stainless steel screw electrodes (2.0 Ø × 0.6 × 1.7 mm; Fukuoka Seimitsu, Fukuoka, Japan) were implanted bilaterally into the frontal cortex (AP: +0.5 mm; ML: ±3.0 mm from bregma) and occipital cortex (AP: −7.0 mm; ML: ±3.0 mm from bregma). In addition, a stainless steel screw implanted into the posterior end of the skull served as a reference electrode. This assembly was fixed to the skull with dental cement (UNIFAST II; GC Dental Products, Aichi, Japan). After a 1-week recovery period, cortical EEG was recorded (Neurofax EEG-1200; Nihon Koden, Tokyo, Japan). The duration of the seizure discharges between seizure onset and termination were analyzed.

Balance-beam test

Each AED has various side effects on the central nervous system, gastrointestinal organs, urinary tracts, and so on, especially following chronic use. In the present study, we assessed only the acute effects on motor coordination and balance because AEDs were administered as a single dose. This test was performed as described previously, with slight modifications (Carter et al., 1999; Perez & Palmiter, 2005). The beam was 105 cm long and 35 mm wide, and it was elevated 100 cm above the ground. A black box (20 × 18 × 30 cm) was set at one end of the beam as the goal. A bright light was situated opposite the goal box to encourage the rats to cross the beam (Fig. 5A). The rats were first trained to traverse the beam and were then tested. Crossing time and the number of footfalls were recorded.

Statistical analysis

Data are presented as mean ± standard error of the mean (SEM). Data analyses were performed using nonrepeated measures analysis of variance (ANOVA) with Dunnett's post hoc test. Seizure severity scores were analyzed using the Kruskal-Wallis *H* test together with the Mann-Whitney *U*-test, followed by the Bonferroni correction post hoc test. Statistical difference was defined as $p < 0.05$.

Results

Effects of AEDs on hyperthermia-induced seizures

In order to evaluate which AEDs are effective against hyperthermia-induced seizures in *Scn1a* mutant rats, we induced seizures by immersing the rats pretreated with each AED in water at 45°C. The anticonvulsant effects of AEDs were assessed using four parameters: incidence of seizure; temperature threshold, calculated from the rectal temperature of the rats immediately after seizure onset; seizure duration; and seizure severity score. DZP and KBr, but no other AEDs, reduced the incidence rate of hyperthermia-induced seizures (Fig. 2A). PB, DZP, TPM, and KBr significantly increased the temperature threshold, whereas CBZ, GBP, and AZA decreased the threshold (Fig. 2B). All AEDs, except CBZ, significantly decreased the seizure duration (Fig. 2C). In particular, AZA, DZP, and KBr shortened the seizure duration dramatically (Fig. 2C). Although DZP and KBr tended to reduce the seizure severity scores, significant changes were not observed (Fig. 2D).

After seizure termination, blood samples were obtained from the tail vein of the rats, and blood concentrations of the AEDs were then measured. Blood concentrations of all AEDs, except those of DZP, increased over the therapeutic range (Table 1). Although the serum level of

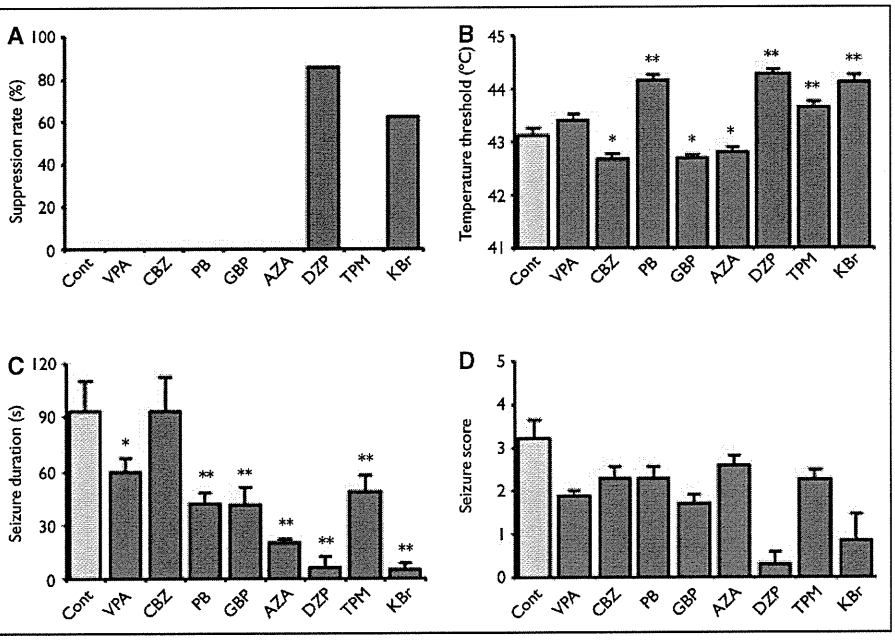

Figure 2.
Comparison of effects of AEDs on hyperthermia-induced seizures in *Scn1a* mutant rats. (**A**) Suppression rate of seizures (%). (**B**) Temperature threshold. Rectal temperature of the rats was measured immediately after seizure onset. (**C**) Seizure duration. (**D**) Seizure severity score. Untreated (Cont., n = 9), VPA-Na (200 mg/kg, n = 8), CBZ (200 mg/kg, n = 7), PB-Na (50 mg/kg, n = 7), GBP (100 mg/kg, n = 7), AZA-Na (55 mg/kg, n = 12), DZP (5 mg/kg, n = 7), TPM (80 mg/kg, n = 8), and KBr (1,800 mg/kg, n = 7). Data are mean ± SEM. *p < 0.05, **p < 0.01 compared to controls (untreated).
Epilepsia © ILAE

Table 1. Blood concentrations of antiepileptic drugs immediately after hyperthermia-induced seizures in *Scn1a* mutant rats

	n	Dose (mg/kg)	Blood level (μg/ml)	Therapeutic range (μg/ml)	References
VPA	8	200	174.7 ± 22.8	40–120	Schmidt, 2009
CBZ	7	200	13.2 ± 1.7	4–12	Eadie, 2001
PB-Na	7	50	40.3 ± 0.8	12–30	Schmidt, 2009
GBP	7	100	33.5 ± 1.4	2–20	McLean, 1999
AZA-Na	12	55	49.8 ± 4.0	10–20	Granero et al., 2007
DZP	7	5	0.15 ± 0.04	0.2–0.6	Ogutu et al., 2002
TPM	8	80	n.d.	–	–
KBr	7	1800	1769.1 ± 204.7	500–1500	Ryan & Baumann, 1999

Data are mean ± SEM.

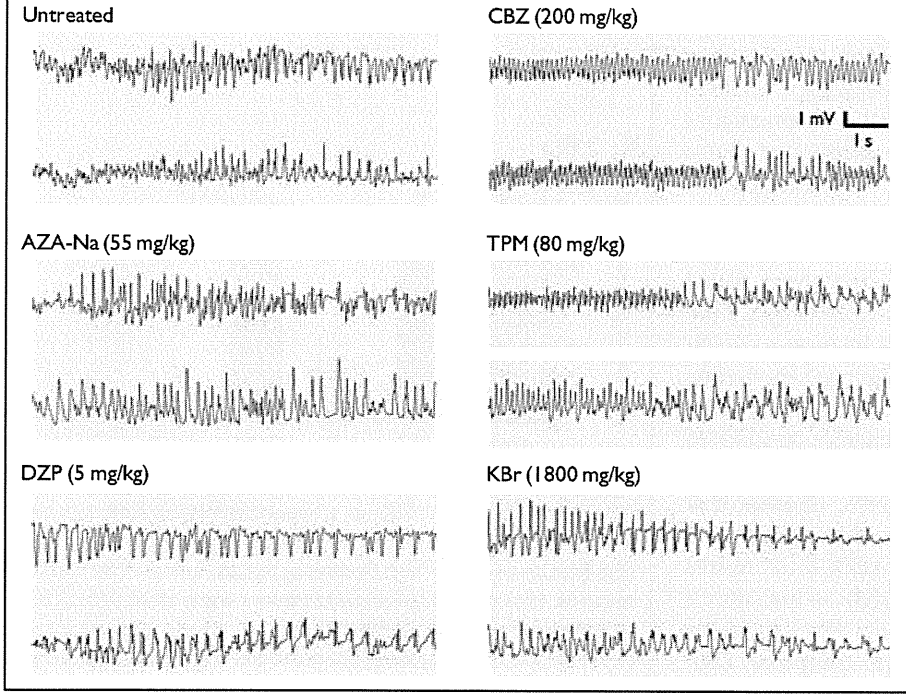

Figure 3.
Representative ictal EEG patterns of a hyperthermia-induced seizure after treatment with each AED. The top and bottom traces were from the frontal and occipital cortices, respectively.
Epilepsia © ILAE

DZP did not reach the therapeutic range in the 5 mg/kg DZP-treated group, these rats showed ataxia and lethargy in the hot bath; therefore, the dose of DZP was not increased. We could not exclude the possibility that higher doses of some of AEDs may have lead to the different results.

Electroencephalography

Ictal EEG patterns were examined in five AEDs (AZA, TPM, DZP, KBr, and CBZ). Representative ictal EEG recordings from the rats are shown in Figs 3 and 4A. It was observed that seizures began as tonic seizures with high frequency spikes, followed by clonic seizures (Fig. 4A). Hyperthermia-induced seizures in *Scn1a* mutant rats were often provoked as several recurrent seizures with a few seconds interval between the seizures. Before the second tonic–clonic seizure occurs, interictal spikes appear and gradually increase their amplitude. Between the first seizure and the second seizure, high amplitude spikes were associated with myoclonic jerks. We analyzed the duration of the seizure discharges on EEGs between seizure onset and termination (Fig. 4A). AZA, DZP, and KBr significantly reduced the duration of the seizure discharges, whereas CBZ and TPM showed no significant changes (Fig. 4B).

Balance-beam test

Motor coordination and balance were examined using the balance-beam test for some of the AEDs which showed remarkable inhibitory effects on hyperthermia-induced seizures (Fig. 5A,B). Although control (i.e., untreated) rats walked along the beam with ease, motor deficits were observed in the PB- and DZP-treated groups (Fig. 5C,D). On the other hand, AZA and KBr did not affect motor coordination or balance (Fig. 5C,D).

Discussion

In total, >600 mutations in the *SCN1A* gene have been identified in patients with SMEI and GEFS+. *SCN1A* is the most representative mutated gene in human fever-related epileptic syndromes. Patients with SMEI have life-threatening status epilepticus, which is often provoked by fever, and patients with GEFS+ have repetitive FS that can persist beyond 6 years. Therefore, induction of appropriate treatments for FS in the early stages of onset is essential for these patients.

Rodent models harboring the responsible mutant genes are often used to elucidate the molecular pathogenesis and to cultivate novel treatments. *Scn1a* KO mice (Yu et al., 2006; Ogiwara et al., 2007) and R1648H-*Scn1a* mice (Martin et al., 2010) were generated to investigate the *SCN1A* gene. Both types of heterozygous mutant mice exhibited susceptibility to hyperthermia-induced seizures (Oakley et al., 2009; Martin et al., 2010). Homozygous N1417H-*Scn1a* mutant rats in the present study also exhibited susceptibility to hyperthermia-induced seizures.

In the present study, the effects of AEDs on hyperthermia-induced seizures were assessed in homozygous N1417H-*Scn1a* mutant rats. DZP and KBr showed potent effects on hyperthermia-induced seizures in these rats. DZP and KBr demonstrated reduction in the incidence of seizures, increase in the temperature threshold, and shortening of the seizure duration. Furthermore, DZP and KBr also decreased the duration of the seizure discharges on EEG. In the balance-beam test, DZP significantly increased the crossing time and total number of footfalls, whereas KBr did not demonstrate a significant effect on these parameters. Together with the blood level of each AED, these results suggested that DZP in low doses, but not KBr in high doses, influences motor coordination and balance. When the pharmacokinetics between DZP and KBr were compared, DZP was shown to be effective in the short term, whereas KBr was shown to have a long half-life (12 days) in blood. Development of tolerance to DZP in long-term treatment is well known (Haigh & Feely, 1988). Given that DZP is the first choice for treatment of status epilepticus because of its potent anticonvulsant effects, prolonged administration of DZP may decrease the effectiveness of stopping seizures in case of status epilepticus. Therefore, KBr may be recommended for repetitive FS.

PB, VPA, and TPM also showed efficacy for preventing hyperthermia-induced seizures. AZA and GBP decreased the seizure threshold but shortened the duration of seizures. However, the molecular mechanisms that induce hyperthermia-induced seizures and terminate seizures remain unknown. The results presented herein suggest that the mechanisms that increase the seizure threshold and terminate seizures are different. Although AZA is used mainly for treating absence seizures, its ability to shorten seizures is remarkable. Hyperthermia-induced respiratory alkalosis involves the onset of hyperthermia-induced seizures (Schuchmann et al., 2006), and metabolic acidosis terminates seizures and prevents seizure progression (Ziemann et al., 2008). AZA, a carbonic anhydrase inhibitor, is known to cause metabolic acidosis. In fact, AZA-Na (55 mg/kg) decreased the peripheral venous blood pH of rats from 7.38 ± 0.01 to 7.22 ± 0.01 within 30 min of oral administration. This acidosis may have been partially responsible

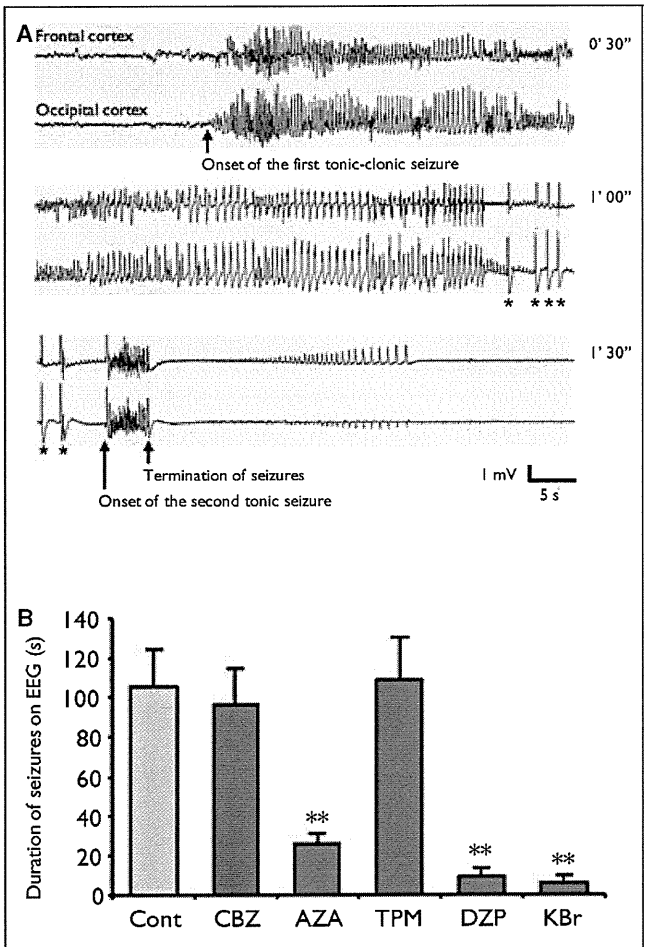

Figure 4.

A representative ictal EEG of a hyperthermia-induced seizure from *Scn1a* mutant rats. (**A**) A seizure began as tonic seizures (the first arrow) with high frequency spikes, followed by clonic seizures. Hyperthermia-induced seizures were often provoked as several recurrent seizures with a few-second interval between the seizures. Before the second tonic seizure occurs (the second arrow), high amplitude spikes were associated with myoclonic jerks. The asterisk (*) indicates myoclonic jerks. After the termination of seizures, repetitive spikes continued for several seconds with no seizure manifestations. (**B**) The duration of the seizure discharges between seizure onset (the first arrow) and termination (the third arrow) was measured. Untreated (Cont., n = 8), CBZ (200 mg/kg, n = 6), AZA-Na (55 mg/kg, n = 7), TPM (80 mg/kg, n = 6), DZP (5 mg/kg, n = 8), and KBr (1,800 mg/kg, n = 7). Data are mean ± SEM. *p < 0.05, **p < 0.01 compared to controls (untreated).

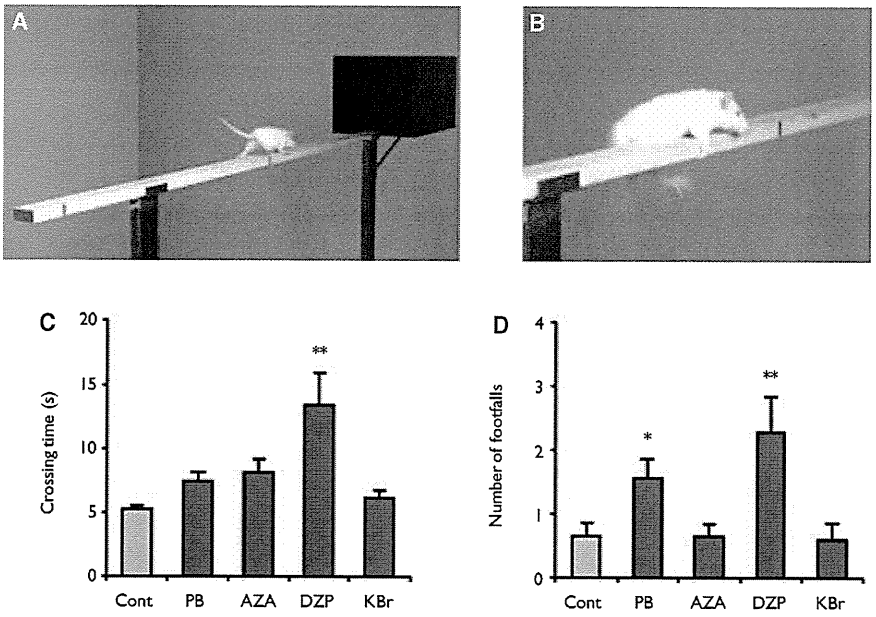

Figure 5.

Balance-beam test apparatus for measuring motor coordination and balance. (**A**) A bright light was placed opposite the black box to encourage the rats to perform the task. The time they took to cross the beam was recorded. (**B**) The number of times the hind limb slipped off the beam was counted. (**C**) Time to cross the beam after treatment with each AED. (**D**) Number of footfalls while crossing the beam after treatment with each AED. Untreated (Cont., n = 14), PB-Na (50 mg/kg, n = 15), AZA-Na (55 mg/kg, n = 14), DZP (5 mg/kg, n = 7), and KBr (1,800 mg/kg, n = 10). Data are mean ± SEM. *p < 0.05, **p < 0.01 compared to controls (untreated).

for decrease in the seizure duration in the AZA-treated group. These findings suggest that AZA is useful for terminating prolonged seizures, but not for inhibiting seizure onset.

Almost all AEDs have a partial effect on hyperthermia-induced seizures. CBZ, on the other hand, significantly reduced the seizure threshold, suggesting that CBZ may aggravate hyperthermia-induced seizures because of its sodium channel blocking effects (Macdonald, 2002).

Taken together, KBr and DZP are first-line treatments for hyperthermia-induced seizures in *Scn1a* mutant rats; PB, TPM, and VPA are second-line treatments. It was observed that AZA suppressed and CBZ aggravated hyperthermia-induced seizures. However, how much of these results in the *Scn1a* mutant rats mimic the results of human epilepsy with *SCN1A* mutation? In patients with SMEI, of which >80% have a mutation in *SCN1A*, benzodiazepines and VPA are effective in preventing seizures (Ceulemans et al., 2004). KBr also improved generalized tonic–clonic seizures, generalized clonic seizures, and complex partial seizures (Oguni et al., 1994). KBr is known to induce several adverse effects such as drowsiness, headache, acneiform rashes, and loss of appetite. The significant toxicity associated with their use and the availability of safer AEDs may lead to a decrease in the use of KBr. The inhibitory effects of TPM as monotherapy were almost equal to those induced by VPA and PB. The clinical efficacy of TPM as adjunctive therapy has been reported in patients with SMEI (Nieto-Barrera et al., 2000, Coppola et al., 2002). Regarding the adverse effects of CBZ in the model rats, CBZ also aggravated seizures in patients with SMEI and GEFS+ (Horn et al., 1986; Guerrini et al., 1998). These reports in humans are consistent with the results presented here in the *Scn1a* mutant rats. *Scn1a* mutant rats seem to reflect considerably the pathogenesis of human *SCN1A* mutation–associated epilepsy. Considering the many differences, such as the way of treatment, treatment dose, type of seizure, age, gender, genetic background, and environmental factors, these rats may be useful for screening new AEDs or novel treatments for FS associated with *SCN1A* mutations in order to predict drugs that might be effective in human patients.

Acknowledgments

We are thankful to Prof. Chiaki Kamei for technical support regarding the EEG recordings. We are thankful to the National Bio Resource Project for the Rat in Japan (http://www.anim.med.kyoto-u.ac.jp/NBR/) for providing rat strains (F344/NSlc-*Scn1a*^{Kyo811}). This work was supported by a Grant-in-Aid from the Ministry of Education, Culture, Sports, Science, and Technology (No. 21390312 to I.O.).

Disclosure

We confirm that we have read the Journal's position on issues involved in ethical publication and affirm that this report is consistent with those guidelines. None of the authors has any conflict of interest to disclose.

References

Baulac S, Gourfinkel-An I, Nabbout R, Huberfeld G, Serratosa J, Leguern E, Baulac M. (2004) Fever, genes, and epilepsy. *Lancet Neurol* 3:421–430.

Borowicz KK, Luszczki JJ, Duda AM, Czuczwar SJ. (2003) Effect of topiramate on the anticonvulsant activity of conventional antiepileptic drugs in two models of experimental epilepsy. *Epilepsia* 44: 640–646.

Carter RJ, Lione LA, Humby T, Mangiarini L, Mahal A, Bates GP, Dunnett SB, Morton AJ. (1999) Characterization of progressive motor deficits in mice transgenic for the human Huntington's disease mutation. *J Neurosci* 19:3248–3257.

Ceulemans B, Boel M, Claes L, Dom L, Willekens H, Thiry P, Lagae L. (2004) Severe myoclonic epilepsy in infancy: toward an optimal treatment. *J Child Neurol* 19:516–521.

Chadman KK, Yang M, Crawley JN. (2009) Criteria for validating mouse models of psychiatric diseases. *Am J Med Genet B Neuropsychiatr Genet* 150B:1–11.

Claes L, Del-Favero J, Ceulemans B, Lagae L, Van Broeckhoven C, De Jonghe P. (2001) De novo mutations in the sodium-channel gene SCN1A cause severe myoclonic epilepsy of infancy. *Am J Hum Genet* 68:1327–1332.

Coppola G, Capovilla G, Montagnini A, Romeo A, Spanò M, Tortorella G, Veggiotti P, Viri M, Pascotto A. (2002) Topiramate as add-on drug in severe myoclonic epilepsy in infancy: an Italian multicenter open trial. *Epilepsy Res* 49:45–48.

Eadie MJ. (2001) Therapeutic drug monitoring – antiepileptic drugs. *Br J Clin Pharmacol* 52(suppl 1):11S–20S.

Granero GE, Longhi MR, Becker C, Junginger HE, Kopp S, Midha KK, Shah VP, Stavchansky S, Dressman JB, Barends DM. (2007) Biowaiver monographs for immediate release solid oral dosage forms: Acetazolamide. *J Pharm Sci* 97:3691–3699.

Guerrini R, Dravet C, Genton P, Belmonte A, Kaminska A, Dulac O. (1998) Lamotrigine and seizure aggravation in severe myoclonic epilepsy. *Epilepsia* 39:508–512.

Haigh JR, Feely M. (1988) Tolerance to the anticonvulsant effect of benzodiazepines. *Trends Pharmacol Sci* 9:361–366.

Hattori J, Ouchida M, Ono J, Miyake S, Maniwa S, Mimaki N, Ohtsuka Y, Ohmori I. (2008) A screening test for the prediction of Dravet syndrome before one year of age. *Epilepsia* 49:626–633.

Hauser WA. (1994) The prevalence and incidence of convulsive disorders in children. *Epilepsia* 35(suppl 2):S1–S6.

Holtzman D, Obana K, Olson J. (1981) Hyperthermia-induced seizures in the rat pup: a model for febrile convulsions in children. *Science* 213:1034–1036.

Horn CS, Ater SB, Hurst DL. (1986) Carbamazepine-exacerbated epilepsy in children and adolescents. *Pediatr Neurol* 2:340–345.

Ishihara K, Kushida H, Yuzurihara M, Wakui Y, Yanagisawa T, Kamei H, Ohmori S, Kitada M. (2000) Interaction of drugs and Chinese herbs: pharmacokinetic changes of tolbutamide and diazepam caused by extract of Angelica dahurica. *J Pharm Pharmacol* 52:1023–1029.

Klauenberg BJ, Sparber SB. (1984) A kindling-like effect induced by repeated exposure to heated water in rats. *Epilepsia* 25:292–301.

Macdonald RL. (2002) Carbamazepine. In Levy RH, Mattson RH, Meldrum BS, Perucca E (Eds) *Antiepileptic drugs*. Lippincott Williams & Wilkins, Philadelphia, pp. 227–235.

Martin MS, Dutt K, Papale LA, Dubé CM, Dutton SB, de Haan G, Shankar A, Tufik S, Meisler MH, Baram TZ, Goldin AL, Escayg A. (2010) Altered function of the SCN1A voltage-gated sodium channel leads to gamma-aminobutyric acid-ergic (GABAergic) interneuron abnormalities. *J Biol Chem* 285:9823–9834.

Mashimo T, Yanagihara K, Tokuda S, Voigt B, Takizawa A, Nakajima R, Kato M, Hirabayashi M, Kuramoto T, Serikawa T. (2008) An ENU-induced mutant archive for gene targeting in rats. *Nat Genet* 40:514–515.

Mashimo T, Ohmori I, Ouchida M, Ohno Y, Tsurumi T, Miki T, Wakamori M, Ishihara S, Yoshida T, Takizawa A, Kato M, Hirabayashi M, Sasa M, Mori Y, Serikawa T. (2010) A missense mutation of the gene encoding voltage-dependent sodium channel (Nav1.1) confers susceptibility to febrile seizures in rats. *J Neurosci* 30:5744–5753.

McLean M. (1999) Gabapentin in the management of convulsive disorders. *Epilepsia* 40(suppl 6):S39–S50; discussion S73–S74.

Nieto-Barrera M, Candau R, Nieto-Jimenez M, Correa A, del Portal LR. (2000) Topiramate in the treatment of severe myoclonic epilepsy in infancy. *Seizure* 9:590–594.

Oakley JC, Kalume F, Yu FH, Scheuer T, Catterall WA. (2009) Temperature- and age-dependent seizures in a mouse model of severe myoclonic epilepsy in infancy. *Proc Natl Acad Sci U S A* 106:3994–3999.

Offringa M, Moyer VA. (2001) Evidence based paediatrics: evidence based management of seizures associated with fever. *BMJ* 323:1111–1114.

Ogiwara I, Miyamoto H, Morita N, Atapour N, Mazaki E, Inoue I, Takeuchi T, Itohara S, Yanagawa Y, Obata K, Furuichi T, Hensch TK, Yamakawa K. (2007) Na(v)1.1 localizes to axons of parvalbumin-positive inhibitory interneurons: a circuit basis for epileptic seizures in mice carrying an Scn1a gene mutation. *J Neurosci* 27:5903–5914.

Oguni H, Hayashi K, Oguni M, Mukahira A, Uehara T, Fukuyama Y, Umezu R, Izumi T, Hara M. (1994) Treatment of severe myoclonic epilepsy in infants with bromide and its borderline variant. *Epilepsia* 35:1140–1145.

Ogutu BR, Newton CR, Crawley J, Muchohi SN, Otieno GO, Edwards G et al. (2002) Pharmacokinetics and anticonvulsant effects of diazepam in children with severe falciparum malaria and convulsions. *Br J Clin Pharmacol* 53:49–57.

Ohmori I, Ouchida M, Ohtsuka Y, Oka E, Shimizu K. (2002) Significant correlation of the SCN1A mutations and severe myoclonic epilepsy in infancy. *Biochem Biophys Res Commun* 295:17–23.

Perez FA, Palmiter RD. (2005) Parkin-deficient mice are not a robust model of parkinsonism. *Proc Natl Acad Sci U S A* 102:2174–2179.

Ryan M, Baumann RJ. (1999) Use and monitoring of bromides in epilepsy treatment. *Pediatr Neurol* 21:523–528.

Scheffer IE, Berkovic SF. (1997) Generalized epilepsy with febrile seizures plus. A genetic disorder with heterogeneous clinical phenotypes. *Brain* 120:479–490.

Schmidt D. (2009) Drug treatment of epilepsy: options and limitations. *Epilepsy Behav* 15:56–65.

Schuchmann S, Schmitz D, Rivera C, Vanhatalo S, Salmen B, Mackie K, Sipilä ST, Voipio J, Kaila K. (2006) Experimental febrile seizures are precipitated by a hyperthermia-induced respiratory alkalosis. *Nat Med* 12:817–823.

Sendrowski K, Sobaniec W, Sobaniec-Lotowska ME, Artemowicz B. (2007) Topiramate as a neuroprotectant in the experimental model of febrile seizures. *Adv Med Sci* 52(suppl 1):161–165.

Ullal GR, Satishchandra P, Shankar SK. (1996) Hyperthermic seizures: an animal model for hot-water epilepsy. *Seizure* 5:221–228.

Verity CM, Butler NR, Golding J. (1985) Febrile convulsions in a national cohort followed up from birth. I – Prevalence and recurrence in the first five years of life. *Br Med J (Clin Res Ed)* 290:1307–1310.

Yu FH, Mantegazza M, Westenbroek RE, Robbins CA, Kalume F, Burton KA, Spain WJ, McKnight GS, Scheuer T, Catterall WA. (2006) Reduced sodium current in GABAergic interneurons in a mouse model of severe myoclonic epilepsy in infancy. *Nat Neurosci* 9:1142–1149.

Ziemann AE, Schnizler MK, Albert GW, Severson MA, Howard MA III, Welsh MJ, Wemmie JA. (2008) Seizure termination by acidosis depends on ASIC1a. *Nat Neurosci* 11:816–822.

Supporting Information

Additional Supporting Information may be found in the online version of this article:

Data S1. Methods.

Figure S1. Comparison of the methods for the induction of hyperthermia-induced seizures in *Scn1a* mutant rats.

Figure S2. Susceptibility of *Scn1a*-N1417H missense mutant rats to water bathing stimuli.

Figure S3. Concentration–time profiles of AEDs after oral administration in 8- to 10-week-old male rats.

Please note: Wiley-Blackwell is not responsible for the content or functionality of any supporting information supplied by the authors. Any queries (other than missing material) should be directed to the corresponding author for the article.

Published in final edited form as:
Nature. ; 478(7367): 114–118. doi:10.1038/nature10490.

Endonuclease G is a novel determinant of cardiac hypertrophy and mitochondrial function

Chris McDermott-Roe[1], **Junmei Ye**[2], **Rizwan Ahmed**[1], **Xi-Ming Sun**[1], **Anna Serafin**[3], **James Ware**[1], **Leonardo Bottolo**[1], **Phil Muckett**[1], **Xavier Cañas**[3], **Jisheng Zhang**[2], **Glenn C. Rowe**[4], **Rachel Buchan**[1], **Han Lu**[1], **Adam Braithwaite**[1], **Massimiliano Mancini**[5], **David Hauton**[6], **Ramon Martí**[7], **Elena García-Arumí**[7], **Norbert Hubner**[8,9], **Howard Jacob**[10], **Tadao Serikawa**[11], **Vaclav Zidek**[12], **Frantisek Papousek**[12], **Frantisek Kolar**[12], **Maria Cardona**[2], **Marisol Ruiz-Meana**[13], **David García-Dorado**[13], **Joan X Comella**[14], **Leanne E Felkin**[15], **Paul JR Barton**[15,16], **Zoltan Arany**[4], **Michal Pravenec**[12], **Enrico Petretto**[1,17], **Daniel Sanchis**[2], and **Stuart A. Cook**[1,16]

[1]Medical Research Council Clinical Sciences Centre, Faculty of Medicine, Imperial College London, Hammersmith Hospital, Du Cane Road, London W12 ONN, UK

[2]Cell Signaling & Apoptosis Group, University Lleida, Biomedical Research Institute of Lleida (IRBLLEIDA), Av Rovira Roure, 80, 25198 Lleida, Spain

[3]Platform of Applied Research on Laboratory Animal Barcelona Science Park, Baldiri Reixac, 4, 08028 Barcelona, Spain

[4]Cardiovascular Institute, Beth Israel Deaconess Medical Institute, CLS906, 3 Blackfan Circle, Boston MA 02215, USA

[5]Department of Radiological, Oncological and Anatomo-Pathological Sciences, Sapienza, University of Rome, Italy

[6]School of Clinical and Experimental Medicine, College of Medical and Dental Sciences, University of Birmingham, Edgbaston, Birmingham, B15 2TT

[7]Unitat de Patologia Mitocondrial i Neuromuscular, Institut de Recerca Hospital Universitari Vall d'Hebron, Universitat Autònoma de Barcelona, Barcelona, Spain

[8]Max-Delbrück Center for Molecular Medicine, Robert-Rössle-Strasse 10, 13125 Berlin, Germany

[9]CC4, Campus Charité Mitte, Charité - Universitätsmedizin Berlin, Charitéplatz 1, 10117 Berlin, Germany

[10]Department of Physiology, Medical College of Wisconsin, Milwaukee WI 53226, U.S.A.

[11]Institute of Laboratory Animals, Graduate School of Medicine, Kyoto University, Yoshidakonoe-cho, Sakyo-ku, Kyoto 606-8501, Japan

[12]Institute of Physiology, Academy of Sciences of the Czech Republic, Vídenska 1083, 142 20 Prague 4, Czech Republic

[13]Grup de Patologia Cardiovascular, Institut de Recerca Hospital Universitari Vall d'Hebron, Universitat Autònoma de Barcelona, Barcelona, Spain

Correspondence and requests: stuart.cook@imperial.ac.uk or daniel.sanchis@cmb.udl.cat .

Author contributions C.M-R, J.Y., X-M.S., A.S., J.Z., A.B., R.B., D.H., H.L., G.C.R., R.M. and E.G-A. performed the lab-based experiments. R.A, P.M., M.M., V.Z., F.P, M.C., M.R-M. and F.K. performed the physiology experiments. N.H., H.J., L.E.F., P.J.R.B. and T.S., provided gene expression and physiology data. J.W, L.B. and E.P. performed genetic mapping and network studies. X.C., J.X.C., Z.A., M.P. and D.C-D. supervised data analysis and contributed to the experimental design. S.A.C and D.S. planned the experiments. S.A.C. wrote the manuscript with input and discussion from all co-authors.